

Onsager-theory-based dynamic model for nematic phases of bent-core molecules and star molecules

Jie Xu¹ and Pingwen Zhang²

¹Department of Mathematics, Purdue University, West Lafayette 47907, USA

²LMAM & School of Mathematical Sciences, Peking University, Beijing 100871, China

Email: xu924@purdue.edu, pzhang@pku.edu.cn

October 12, 2018

Abstract

We construct the molecular model and the tensor model for the dynamics of the nematic phases of bent-core molecules and star molecules in incompressible fluid. We start from the molecular interaction and the molecule–fluid friction, and write down a general formulation based on the molecular shape and the free energy. Then we incorporate an Onsager-theory-based static tensor model that is determined by the molecular shape. In this way, the terms in the molecular model are fully determined by the molecular shape and expressed by physical parameters. For bent-core molecules and star molecules, the model shares the same form, but is different in the coefficients. With the polar interaction and elastic energy taken into account, and the convection and diffusion included both spatially and orientationally, the model is suitable for inhomogeneous flows. We adopt the quasi-equilibrium approximation to derive the tensor model with energy dissipation maintained. Numerical simulation is carried out focusing on the shear flow problem using both the molecular and the tensor models. We choose the parameters near the transition region of different equilibrium nematic phases and examine the effect of molecular shape on the flow modes. The tensor model proves to exhibit all the flow modes found in the molecular model.

Keywords: liquid crystals; hydrodynamics; kinetic theory; tensor model; quasi-equilibrium closure approximation; bent-core molecules; star molecules.

1 Introduction

The liquid crystalline flows are studied extensively in the last few decades. The majority of works focus rod-like molecules that can exhibit uniaxial nematic phase in equilibrium. The earliest and simplest approach is the macroscopic Ericksen-Leslie theory [22]. However, this approach is insufficient to investigate singular phenomena, such as defects. For the microscopic approach, Doi [10] established the kinetic equation of the density function (the Smoluchowski equation), which we call the molecular model. Doi theory has been applied to study the spatially homogeneous shear flow problem for rod-like molecules [12, 13, 20, 21]. It has also been extended to inhomogeneous flows [14, 25, 36, 41, 42]. Despite its great success, the simulation is time-consuming, making its application to inhomogeneous flows

rather restricted. To reduce the dimension of variables, many works aim to construct models in which the orientation is described by tensors. Apart from some phenomenological tensor models [4, 27], most tensor models are obtained by closure approximation of Doi theory [2, 3, 8, 11, 17, 18, 19, 35, 40]. With various closure approximations for different types of flows, the tensor models have proved to be able to capture the phenomena in the molecular model, although no one closure approximation can recover all the phenomena. The Doi theory, the tensor models and the Ericksen-Leslie theory have been shown closely bonded [16].

When the molecule is not axisymmetric, it is possible to exhibit multiple nematic phases. As a representative, bent-core molecules have attracted much attention. Besides the uniaxial nematic phase, they have proved to be able to show the biaxial nematic phase [1, 24], and the twist-bend phase [6, 9, 26], a modulated nematic phase with polar order. The phase behavior of bent-core molecules has also been discussed theoretically [5, 15, 29, 30, 34]. The dynamics of bent-core molecules is expected to be much more complicated and fascinating. However, the works on the dynamics of non-axisymmetric liquid crystals are sparse. Macroscopic dynamic models have been proposed for the biaxial nematic phase [7, 23, 28] as an extension of the Ericksen-Leslie theory. But their applications are even more limited than the Ericksen-Leslie theory since multiple nematic phases may coexist. As for the microscopic approaches, the Smoluchowski equation is adopted to investigate the dynamics of ellipsoids [32, 33] and bent-core molecules [31]. These works focus on the homogeneous shear flow problem and have obtained flow modes different from rod-like molecules. Nevertheless, since the equilibrium theory of bent-core molecules was far from well-established at the time these works were carried out, the model in these works includes only the local biaxial interaction. This makes the model only specifically suitable for the homogeneous flows, because the polar interaction and modulation have proved to be crucial in inhomogeneous systems. In addition, the terms in their model are derived from different molecular architectures. This inconsistency blurs the effect of molecular shape on the flow features, which would be the most interesting problem to be studied.

In a recent work [38], we construct a static tensor model from the Onsager theory for the nematic phases of bent-core molecules and star molecules (see Fig. 1). We assume that the molecule is rigid and consists of spheres. The free energy is a functional of three tensors, one first-order (vector) and two second-order symmetric, with gradient terms included, enabling the free energy to describe polarity and modulation. The form of the free energy is determined by molecular symmetry, and the coefficient of each term is derived as a function of physical parameters. In this work, we build the free energy into the dynamic model. To incorporate the molecule-fluid interaction, we adopt the same molecular architecture in the static model and consider the friction between the fluid and spheres. In this way, we are able to write down the molecular model, with the energy dissipation law, fully based on molecular architecture and physical parameters. Similar to the static model, for bent-core molecules and star molecules, the model shares the same form, but different in coefficients. The model includes convection terms that originate from the molecular-fluid interaction, and diffusion terms that originate from molecular interaction, both spatially and orientationally. Together with the polarity and modulation, the model is applicable to inhomogeneous flows. We then write down the tensor model by deriving the equation of the three tensors appearing in the free energy from the Smoluchowski equation. The high-order tensors appearing in the tensor model are expressed by the three tensors using quasi-equilibrium approximation, a generalization of the Bingham

closure. When adopting the quasi-equilibrium approximation, the tensor model retains the energy dissipation law.

For the numerical simulation, we restrained our attention to the shear flow problem. In particular, we choose the parameters in the vicinity of the uniaxial-biaxial phase boundary, which is not studied previously. We focus on adjusting the parameters describing the molecular shape, and investigate how the flow modes are altered. Also, we compare the results from the molecular model and the tensor model. The tensor model is able to exhibit all the flow modes found in the molecular model, although under different parameters.

The paper is organized as follows. In Sec. 2 we derive the molecular model. In Sec. 3 we derive the tensor model and prove the energy dissipation along with the quasi-equilibrium closure approximation. In Sec. 4 we use both molecular model and tensor model to examine the shear flow problem. A conclusion is drawn in Sec. 5.

2 Molecular model

2.1 Notations

We view the molecules that form liquid crystalline states as fully rigid. Thus, we may choose a body-fixed orthogonal frame $(\hat{O}; \mathbf{m}_1, \mathbf{m}_2, \mathbf{m}_3)$ to describe the position and the orientation of a molecule. In a space-fixed orthogonal coordinate system $(O; \mathbf{e}_1, \mathbf{e}_2, \mathbf{e}_3)$, they can be expressed in terms of $\mathbf{x} = \overrightarrow{O\hat{O}}$ and a three-dimensional proper rotation $P \in SO_3$. In the language of matrix, P is a 3×3 orthogonal with $\det P = 1$ such that

$$(\mathbf{m}_1, \mathbf{m}_2, \mathbf{m}_3) = (\mathbf{e}_1, \mathbf{e}_2, \mathbf{e}_3)P. \quad (2.1)$$

The elements of $P^T = (m_{ij})$ are the components of \mathbf{m}_i , denoted by

$$m_{ij} = \mathbf{m}_i \cdot \mathbf{e}_j.$$

In some cases, we need to specify a point on the molecule, and we use its coordinates $\hat{\mathbf{r}}$ in the body-fixed frame $(\hat{O}; \mathbf{m}_1, \mathbf{m}_2, \mathbf{m}_3)$. Every $P \in SO_3$ can be expressed by Euler angles α, β, γ :

$$P(\alpha, \beta, \gamma) = \begin{pmatrix} \cos \alpha & -\sin \alpha \cos \gamma & \sin \alpha \sin \gamma \\ \sin \alpha \cos \beta & \cos \alpha \cos \beta \cos \gamma - \sin \beta \sin \gamma & -\cos \alpha \cos \beta \sin \gamma - \sin \beta \cos \gamma \\ \sin \alpha \sin \beta & \cos \alpha \sin \beta \cos \gamma + \cos \beta \sin \gamma & -\cos \alpha \sin \beta \sin \gamma + \cos \beta \cos \gamma \end{pmatrix}, \quad (2.2)$$

with

$$\alpha \in [0, \pi], \quad \beta, \gamma \in [0, 2\pi).$$

The uniform probability measure on SO_3 is given by

$$d\nu = \frac{1}{8\pi^2} \sin \alpha d\alpha d\beta d\gamma.$$

For the notations of tensors, we use the summation over repeated indices. The product of several tensors without operators is recognized as tensor product: $\mathbf{m}_1\mathbf{m}_2\mathbf{m}_3$ represents a

third order tensor with the (i, j, k) component $m_{1i}m_{2j}m_{3k}$. If a tensor contraction involves first or second order tensor, we also use the single and double dots: suppose we have a first order tensor \mathbf{p} , a second order tensor Q , and a fourth order tensor R , then

$$(Q \cdot \mathbf{p})_i = Q_{ij}p_j, \quad (\mathbf{p} \cdot R)_{jkl} = p_i R_{ijkl}, \quad (Q : R)_{kl} = Q_{ij}R_{ijkl}. \quad (2.3)$$

To describe the number of molecules with certain position \mathbf{x} and orientation P , we introduce the density function $f(\mathbf{x}, P)$. Moreover, we split $f(\mathbf{x}, P)$ into the local concentration $c(\mathbf{x})$ and the orientational distribution $\rho(\mathbf{x}, P)$,

$$c(\mathbf{x}) = \int d\nu f(\mathbf{x}, P), \quad \rho(\mathbf{x}, P) = f(\mathbf{x}, P)/c(\mathbf{x}). \quad (2.4)$$

The notation $\langle \cdot \rangle$ represents the average about $\rho(\mathbf{x}, P)$,

$$\langle (\cdot) \rangle = \int d\nu (\cdot) \rho(\mathbf{x}, P).$$

The differential operators on $SO(3)$ are involved when discussing the motion of the rigid molecules. In specific, we use L_i to denote the derivatives along the infinitesimal rotation about \mathbf{m}_i . The operators L_i can be expressed by derivatives of Euler angles,

$$L_1 = \frac{\partial}{\partial \gamma}, \quad (2.5)$$

$$L_2 = \frac{-\cos \gamma}{\sin \alpha} \left(\frac{\partial}{\partial \beta} - \cos \alpha \frac{\partial}{\partial \gamma} \right) + \sin \gamma \frac{\partial}{\partial \alpha}, \quad (2.6)$$

$$L_3 = \frac{\sin \gamma}{\sin \alpha} \left(\frac{\partial}{\partial \beta} - \cos \alpha \frac{\partial}{\partial \gamma} \right) + \cos \gamma \frac{\partial}{\partial \alpha}. \quad (2.7)$$

Denote $L = (L_1, L_2, L_3)^T$. If a vector-valued function $\mathbf{a}(P)$ is expressed as $\mathbf{a}(P) = a_1(P)\mathbf{m}_1 + a_2(P)\mathbf{m}_2 + a_3(P)\mathbf{m}_3$, then the divergence is defined by

$$L \cdot \mathbf{a} = L_1 a_1 + L_2 a_2 + L_3 a_3.$$

We may verify the following properties using the above definition. Acting the operators on m_{ij} , we have

$$L_i \mathbf{m}_j = \epsilon_{ijk} \mathbf{m}_k. \quad (2.8)$$

Here we use the Levi-Civita symbol,

$$\epsilon_{k_1 k_2 k_3} = \begin{cases} 1, & (k_1 k_2 k_3) = (123), (231), (312); \\ -1, & (k_1 k_2 k_3) = (132), (213), (321); \\ 0, & \text{otherwise.} \end{cases}$$

The operators also satisfy the integration by parts on $SO(3)$,

$$\int d\nu f(L_i g) = - \int d\nu (L_i f) g. \quad (2.9)$$

2.2 General formulation

The motion of rigid molecules includes translation and rotation, driven by molecular interaction and molecule–fluid interaction. In general, the translation and rotation can be coupled. But in what follows, we will deduce them separately under various approximations. To let our discussion be specific, we assume that a rigid molecule consists of spheres of the diameter D and the mass m_0 . In this case, the architecture of a molecule is given by the number density of the sphere centers $\hat{\rho}(\hat{\mathbf{r}})$ in the body fixed frame $(\hat{O}; \mathbf{m}_1, \mathbf{m}_2, \mathbf{m}_3)$, and we assume that the center of mass is located at \hat{O} . The rigid molecules are dissolved in incompressible viscous fluid, and the molecule–fluid interaction stems from the friction between them. The frictional force between a sphere and the fluid is proportional to the relative velocity, given by $\mathbf{F} = -\zeta \mathbf{V}$, where $\zeta = 3\pi D\eta_0$ is the friction constant.

The molecular interaction induces a potential field $\mu(\mathbf{x}, P)$ given by the functional derivative

$$\mu = \frac{\delta F[f]}{\delta f}, \quad (2.10)$$

where $F[f]$ represents the free energy of a system with the number density $f(\mathbf{x}, P)$ of rigid molecules. The free energy includes the contribution of the entropy and pairwise interaction,

$$F[f] = F_{entropy}[f] + F_r[f], \quad (2.11)$$

where

$$F_{entropy} = k_B T \int d\mathbf{x} d\nu f \log f. \quad (2.12)$$

For bent-core molecules and star molecules, we will give the expression of F_r later.

2.2.1 Smochulowski equation

In general, the Smochulowski equation for the rigid molecules can be written as

$$\frac{\partial f}{\partial t} = -\nabla \cdot (f\mathbf{w}) - L \cdot (f\boldsymbol{\omega}). \quad (2.13)$$

Here, for the molecule at the position \mathbf{x} and the orientation P , we use $\mathbf{w}(\mathbf{x}, P)$ to denote the velocity of the center of mass, and $\boldsymbol{\omega}(\mathbf{x}, P)$ to denote the angular velocity. For both of them, we split the contribution of molecular interaction, $\mathbf{w}_m, \boldsymbol{\omega}_m$, and fluid–molecule interaction, \mathbf{w}_f, \mathbf{g} , by writing

$$\mathbf{w} = \mathbf{w}_m + \mathbf{w}_f, \quad \boldsymbol{\omega} = \boldsymbol{\omega}_m + \mathbf{g}.$$

We start from the rotation resulted from the molecular interaction. To derive this term, we assume that a molecule is rotating in the quiescent fluid, with the angular velocity $\boldsymbol{\omega}_m$ round the center of mass. The torque generated by the friction between a molecule and the quiescent fluid is the sum of frictional torque on each sphere,

$$-\mathbf{N} = \zeta \int d\hat{\mathbf{r}} \hat{\rho}(\hat{\mathbf{r}}) \hat{\mathbf{r}} \times (\boldsymbol{\omega}_m \times \hat{\mathbf{r}}) = \frac{\zeta}{m_0} \mathbf{I} \boldsymbol{\omega}_m, \quad (2.14)$$

where \mathbf{I} is the moment of inertia of a molecule, calculated as

$$\mathbf{I} = m_0 \int d\hat{\mathbf{r}} \hat{\rho}(\hat{\mathbf{r}}) (|\hat{\mathbf{r}}|^2 - \hat{\mathbf{r}}\hat{\mathbf{r}}). \quad (2.15)$$

On the other hand, suppose the molecule is doing an infinitesimal rotation $\delta P = \delta t \boldsymbol{\phi} \times P$. Then the work done by the frictional torque is $-\mathbf{N} \cdot \boldsymbol{\phi} \delta t$, and shall equal to the variation of potential. Therefore,

$$\mathbf{N} \cdot \boldsymbol{\phi} \delta t = \mu(P + \delta P) - \mu(f) = \delta t \boldsymbol{\phi} \cdot L\mu,$$

yielding $\mathbf{N} = L\mu$. Comparing it with (2.14), we have

$$\boldsymbol{\omega}_m = -\frac{m_0}{\zeta} \mathbf{I}^{-1} L\mu.$$

If we carefully choose \mathbf{m}_i such that \mathbf{I} is diagonal in the body-fixed frame, then we can write

$$\boldsymbol{\omega}_m = \sum_{i=1}^3 \omega_i \mathbf{m}_i = -\sum_{i=1}^3 (D_i L_i \mu) \mathbf{m}_i,$$

where the diffusion coefficients are given by

$$D_i = \frac{m_0}{\zeta I_{ii}}. \quad (2.16)$$

Note that $\boldsymbol{\omega}_m$ actually gives a diffusion term $L \cdot (m_0 \zeta^{-1} \mathbf{I}^{-1} f L \mu)$ in the Smoluchowski equation. Define

$$V = \frac{\delta F_r}{\delta f}, \quad (2.17)$$

then we can split μ as

$$\mu = k_B T (\log f + 1) + V. \quad (2.18)$$

and the diffusion term can also be written as

$$\sum_{i=1}^3 D_i [k_B T L_i^2 f + L_i (f L_i V)]. \quad (2.19)$$

Similarly, we derive \mathbf{w}_m by considering the translation of a molecule in the quiescent fluid. Generally, \mathbf{w}_m can be written as

$$\mathbf{w}_m = -\mathbf{J} (k_B T \nabla f + f \nabla V), \quad (2.20)$$

where the diffusion coefficient \mathbf{J} is a 3×3 positive matrix. To derive \mathbf{J} , we need to consider the hydrodynamic interaction, namely the interaction of different spheres through the fluid, which can be done using the Kirkwood theory (see [10]). In Appendix, we will outline how to use the Kirkwood theory to calculate \mathbf{J} and present the result for bent-core molecules. As a simple approximation, if we ignore the hydrodynamic interaction, then \mathbf{J} will be a multiple of the identity matrix.

Next we derive the translation and rotation generated by molecule–fluid interaction. Now we need to consider the motion of a molecule driven by the fluid with inhomogeneous velocity. We require that the velocity of the center of mass, \mathbf{w}_f , and the angular velocity, \mathbf{g} , minimize the frictional work. Denote by $\mathbf{u}(\hat{\mathbf{r}})$ and $\mathbf{u}_p(\hat{\mathbf{r}})$ the velocity of the fluid and the sphere at the point $\hat{\mathbf{r}}$, respectively. Then the frictional work of the fluid and the molecule can be written as

$$W = \zeta \int d\hat{\mathbf{r}} \hat{\rho}(\hat{\mathbf{r}}) |\mathbf{u} - \mathbf{u}_p|^2. \quad (2.21)$$

Note that $\mathbf{u}_p = \mathbf{w}_f - \mathbf{g} \times \hat{\mathbf{r}}$. Since the scale of rigid molecule is much smaller than the fluid field, we may suppose that the flow is linear. In other words, if we denote $\kappa_{ij} = \partial_j u_i$, then we may assume

$$\mathbf{u}(\hat{\mathbf{r}}) = \kappa \cdot \hat{\mathbf{r}} + \mathbf{u}_0.$$

Here, \mathbf{u}_0 is the velocity at \mathbf{x} , where \hat{O} is located. By minimizing (2.21), we deduce that

$$\mathbf{w}_f = \mathbf{u}_0, \quad \mathbf{g} = m_0 \mathbf{I}^{-1} \int d\hat{\mathbf{r}} \hat{\rho}(\hat{\mathbf{r}}) (\hat{\mathbf{r}} \times \kappa \cdot \hat{\mathbf{r}}). \quad (2.22)$$

If we denote the fluid velocity by $\mathbf{v}(\mathbf{x})$, then we may write

$$\mathbf{w}_f = \mathbf{u}_0 = \mathbf{v}. \quad (2.23)$$

Summarizing the derivation above, the Smoluchowski equation can be rewritten as follows,

$$\frac{\partial f}{\partial t} + \nabla \cdot (f\mathbf{v}) = \nabla \cdot (\mathbf{J}(k_B T \nabla f + f \nabla V)) + L \cdot [(D_0 \mathbf{I}^{-1})(k_B T L f + f L V)] - L \cdot (\mathbf{g} f). \quad (2.24)$$

2.2.2 Momentum equation

The incompressibility gives

$$\nabla \cdot \mathbf{v} = 0. \quad (2.25)$$

The momentum equation is written as

$$\rho_s \left(\frac{\partial \mathbf{v}}{\partial t} + \mathbf{v} \cdot \nabla \mathbf{v} \right) = -\nabla p + \nabla \cdot \tau + \mathbf{F}_e, \quad (2.26)$$

where ρ_s is the density of the fluid, \mathbf{F}_e is the external force, and $\tau = \tau_e + \tau_v$ is the stress, divided into the elastic and the viscous part. The elastic stress τ_e and the external force \mathbf{F}_e can be derived from the principle of virtual work. Because the derivation is standard and can be found in literature [10, 31], we only list the results here. The external force \mathbf{F}_e is given by

$$\mathbf{F}_e = - \int d\nu \nabla \mu(f) f = -c \langle \nabla \mu \rangle, \quad (2.27)$$

where we recall that c is the concentration. For τ_e , if we express \mathbf{g} as

$$\mathbf{g} = \kappa_{jk} : (\alpha_i)_{jk} \mathbf{m}_i, \quad (2.28)$$

then

$$(\tau_e)_{jk} = c \langle (\alpha_i)_{jk} L_i \mu \rangle. \quad (2.29)$$

When \mathbf{I} is diagonal, by (2.22), we deduce

$$\alpha_i = m_0 I_{ii}^{-1} \int d\hat{\mathbf{r}} \hat{\rho}(\hat{\mathbf{r}}) \hat{\mathbf{r}} (\mathbf{m}_i \times \hat{\mathbf{r}}). \quad (2.30)$$

The viscous stress can be expressed as

$$\tau_v = 2\eta(\kappa + \kappa^T) + \tau_{vf}. \quad (2.31)$$

The first term is the contribution of the friction in the fluid itself, and τ_{vf} is the contribution of the friction between the fluid and the molecules, determined by the following equation

$$c\langle W \rangle = \kappa : \tau_{vf}, \quad (2.32)$$

where W is given by (2.21) with \mathbf{g} taking (2.22).

The whole system is described by (2.24)-(2.26), with the terms given by (2.16), (2.22), (2.27), (2.29), (2.32). It is worth noting that all the terms are derived from the distribution of sphere centers $\hat{\rho}(\hat{\mathbf{r}})$ and the free energy $F[f]$.

2.2.3 Energy dissipation law

The energy of the system includes the free energy (2.11) and the kinetic energy of the fluid,

$$\int d\mathbf{x} \frac{\rho_s}{2} |\mathbf{v}|^2 + F[f].$$

Now let us prove the energy dissipation law. For simplicity, we omit $k_B T$ in the following. We have

$$\begin{aligned} & \frac{d}{dt} \left(\int d\mathbf{x} \frac{\rho_s}{2} |\mathbf{v}|^2 + F[f] \right) = \int d\mathbf{x} \left(\rho_s \mathbf{v} \cdot \frac{\partial \mathbf{v}}{\partial t} + \int d\nu \mu \frac{\partial f}{\partial t} \right) \\ &= \int d\mathbf{x} \left[\int d\nu \mu L \cdot (D_0 \mathbf{I}^{-1} f L \mu) + \mu \nabla \cdot (\mathbf{J} f \nabla \mu) - \mu L \cdot (\mathbf{g} f) - \mu \nabla \cdot (\mathbf{v} f) \right] \\ & \quad - \rho_s \mathbf{v} \cdot (\mathbf{v} \cdot \nabla) \mathbf{v} - \mathbf{v} \cdot \nabla p + \mathbf{v} \cdot (\nabla \cdot \boldsymbol{\tau}) + \mathbf{v} \cdot \mathbf{F}_e \\ &= \int d\mathbf{x} \left[\int d\nu - f (L \mu)^T D_0 \mathbf{I}^{-1} (L \mu) - f (\nabla \mu)^T \mathbf{J} (\nabla \mu) + f \mathbf{g} \cdot L \mu + \mathbf{v} \cdot f \nabla \mu \right] \\ & \quad + \frac{\rho_s}{2} (\nabla \cdot \mathbf{v}) |\mathbf{v}|^2 + p \nabla \cdot \mathbf{v} - \kappa : (\boldsymbol{\tau}_e + \boldsymbol{\tau}_f) + \mathbf{v} \cdot \mathbf{F}_e \\ &= \int d\mathbf{x} \left[\int d\nu - f (L \mu)^T D_0 \mathbf{I}^{-1} (L \mu) - f (\nabla \mu)^T \mathbf{J} (\nabla \mu) \right. \\ & \quad \left. + (f \mathbf{g} \cdot L \mu - f (\kappa : \alpha_j) L_j \mu) + (\mathbf{v} \cdot f \nabla \mu - \mathbf{v} \cdot c \rho \nabla \mu) \right] - \kappa : \boldsymbol{\tau}_f \\ &= \int d\mathbf{x} \left[- \langle (L \mu)^T D_0 \mathbf{I}^{-1} (L \mu) \rangle - \langle (\nabla \mu)^T \mathbf{J} (\nabla \mu) \rangle - 2\eta \frac{\kappa + \kappa^T}{2} : \frac{\kappa + \kappa^T}{2} - \kappa : \boldsymbol{\tau}_{vf} \right]. \quad (2.33) \end{aligned}$$

In the above, we ignore the boundary terms. Note that the first three terms are not positive. By (2.32) and (2.21) we know that the last term is not positive either.

2.3 Bent-core molecules and star molecules

For bent-core molecules and star molecules, the sphere centers are distributed in the plane $\hat{O} \mathbf{m}_1 \mathbf{m}_2$. In this case, we can simplify the expressions derived above. First, we have $I_{33} = I_{11} + I_{22}$. Thus, in (2.22),

$$\mathbf{g} = (\kappa : \mathbf{m}_2 \mathbf{m}_3) \mathbf{m}_1 - (\kappa : \mathbf{m}_1 \mathbf{m}_3) \mathbf{m}_2 + \frac{1}{I_{11} + I_{22}} (I_{22} \kappa : \mathbf{m}_1 \mathbf{m}_2 - I_{11} \kappa : \mathbf{m}_2 \mathbf{m}_1) \mathbf{m}_3. \quad (2.34)$$

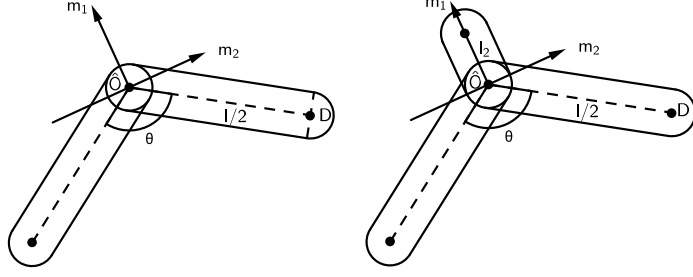


Fig. 1: Bent-core molecule and star molecule.

Then in (2.29), we have

$$\alpha_1 = \mathbf{m}_2 \mathbf{m}_3, \quad \alpha_2 = -\mathbf{m}_1 \mathbf{m}_3, \quad \alpha_3 = \frac{1}{I_{11} + I_{22}} (I_{22} \mathbf{m}_1 \mathbf{m}_2 - I_{11} \mathbf{m}_2 \mathbf{m}_1). \quad (2.35)$$

By (2.21) and (2.32), we deduce that

$$\begin{aligned} \tau_{vf} = \frac{c\zeta\kappa}{m_0} : & \left[I_{22} \langle \mathbf{m}_1 \mathbf{m}_1 \mathbf{m}_1 \mathbf{m}_1 \rangle + I_{11} \langle \mathbf{m}_2 \mathbf{m}_2 \mathbf{m}_2 \mathbf{m}_2 \rangle \right. \\ & \left. + \frac{I_{11} I_{22}}{I_{11} + I_{22}} \langle (\mathbf{m}_1 \mathbf{m}_2 + \mathbf{m}_2 \mathbf{m}_1)(\mathbf{m}_1 \mathbf{m}_2 + \mathbf{m}_2 \mathbf{m}_1) \rangle \right]. \end{aligned} \quad (2.36)$$

We can see that the only difference in the above terms lies in the coefficients as functions of the moment of inertia, from which we can distinguish the bent-core molecules and star molecules. For a bent-core molecule (drawn in Fig. 1 left), the sphere centers are distributed uniformly and continuously on a two-segment broken line, where the length of each segment is $l/2$. Thus, $\hat{\rho}$ is given by

$$\hat{\rho}(\hat{\mathbf{r}}) = \frac{1}{l} \int_{-\frac{l}{2}}^{\frac{l}{2}} ds \delta\left(\hat{\mathbf{r}} - \left(\frac{l}{4} - |s|\right) \cos \frac{\theta}{2} \mathbf{m}_1 - s \sin \frac{\theta}{2} \mathbf{m}_2\right). \quad (2.37)$$

Substituting it into (2.15) and recalling (2.16), we obtain

$$I_{11} = \frac{l^2 m_0}{48} \cdot 4 \sin^2 \frac{\theta}{2}, \quad I_{22} = \frac{l^2 m_0}{48} \cdot \cos^2 \frac{\theta}{2}. \quad (2.38)$$

For a star molecule (drawn in Fig. 1 right), the sphere centers also lie in a third line segment of the length l_2 . Thus, $\hat{\rho}$ is given by

$$\hat{\rho}(\hat{\mathbf{r}}) = \frac{1}{l + l_2} \left[\int_{-\frac{l}{2}}^{\frac{l}{2}} ds \delta\left(\hat{\mathbf{r}} - \left(\frac{l}{4} - |s|\right) \cos \frac{\theta}{2} \mathbf{m}_1 - s \sin \frac{\theta}{2} \mathbf{m}_2\right) + \int_0^{l_2} ds \delta(\hat{\mathbf{r}} - s \mathbf{m}_1) \right]. \quad (2.39)$$

Therefore,

$$I_{11} = \frac{l^2 m_0}{12} \sin^2 \frac{\theta}{2}, \quad I_{22} = m_0 \left(\frac{\frac{1}{3} l_2^3 + \frac{1}{12} l^3 \cos^2 \frac{\theta}{2}}{l + l_2} - x_C^2 \right), \quad (2.40)$$

where

$$x_C = \frac{\frac{1}{2} l_2^2 - \frac{1}{4} l^2 \cos \frac{\theta}{2}}{l + l_2}$$

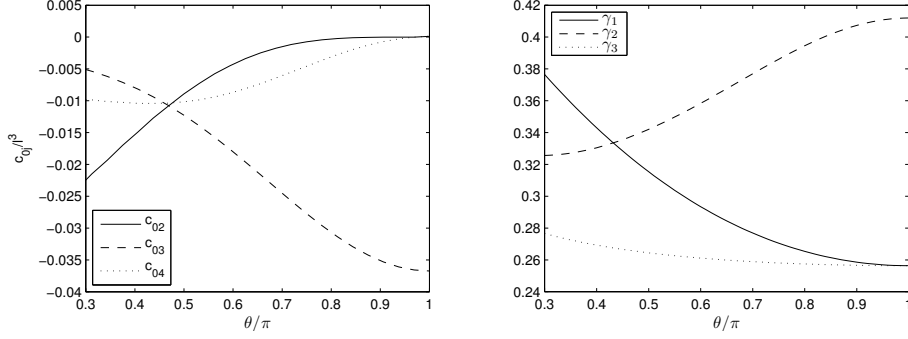


Fig. 2: Some coefficients in the model for bent-core molecules with $D/l = 1/40$. Left: coefficients of the bulk energy. Right: translational diffusion coefficients.

is the \mathbf{m}_1 -coordinate of the center of mass.

For bent-core molecules and star molecules, the spatial diffusion matrix \mathbf{J} derived from the Kirkwood theory (see Appendix) is diagonal in the frame (\mathbf{m}_i) ,

$$\mathbf{J} = \frac{1}{8\pi D\eta_0} \sum_{j=1}^3 \gamma_j \mathbf{m}_j \mathbf{m}_j. \quad (2.41)$$

For bent-core molecules with $D/l = 1/40$, we plot γ in Fig. 2 right.

For the free energy, we adopt the tensor model derived in [38] from the second virial expansion with the hardcore molecular interaction. The hardcore interaction is determined only by the molecular shape, given by $\hat{\rho}$ in the current context. Assume that the concentration c is constant. Define $\mathbf{p} = \langle \mathbf{m}_1 \rangle$, $Q_1 = \langle \mathbf{m}_1 \mathbf{m}_1 \rangle$, $Q_2 = \langle \mathbf{m}_2 \mathbf{m}_2 \rangle$. For both molecules, F_r shares the form below,

$$\begin{aligned} \frac{F_r}{k_B T} = & \int d\mathbf{x} \frac{c^2}{2} (c_{01} |\mathbf{p}|^2 + c_{02} |Q_1|^2 + c_{03} |Q_2|^2 + 2c_{04} Q_1 : Q_2) \\ & + c^2 (c_{11} p_j \partial_i Q_{1ij} + c_{12} p_j \partial_i Q_{2ij}) \\ & + \frac{c^2}{4} [c_{21} |\nabla \mathbf{p}|^2 + c_{22} |\nabla Q_1|^2 + c_{23} |\nabla Q_2|^2 + 2c_{24} \partial_i Q_{1jk} \partial_i Q_{2jk} \\ & + 2c_{27} \partial_i p_i \partial_j p_j + 2c_{28} \partial_i Q_{1ik} \partial_j Q_{1jk} + 2c_{29} \partial_i Q_{2ik} \partial_j Q_{2jk} + 4c_{2,10} \partial_i Q_{1ik} \partial_j Q_{2jk}], \end{aligned} \quad (2.42)$$

which is determined by the molecular symmetry [38, 39]. The difference also lies in the coefficients c_{kj} . They are derived as functions of the molecular parameters l , D , θ for bent-core molecules, and also l_2 for star molecules. They possess the scaling property

$$c_{kj} = l^{k+3} \tilde{c}_{kj}(D/l, \theta, l_2/l). \quad (2.43)$$

The calculation of c_{kj} is discussed in [38, 39]. In Fig. 2 left we plot c_{02}, c_{03}, c_{04} that are necessary for the shear flow problem.

To summarize, we establish the dynamic model from the molecular shape described by $\hat{\rho}$, and the free energy $F[f]$. In the case of hardcore interaction, $F[f]$ is also determined by the

molecular shape. Therefore, the model is able to characterize the dynamics of molecules with different shapes. In particular, for bent-core molecules and star molecules, the model has the same form, no matter for the free energy F and other terms. The two types of molecules are distinguished by numerous coefficients in the model, which are expressed as functions of molecular parameters.

3 Tensor model

We derive the tensor model from the molecular model. When we use the free energy (2.42), the elastic stress τ_e and the external force \mathbf{F}_e can also be expressed by tensors. Let V be computed from the free energy (2.42). Denote

$$V_{\mathbf{p}} = \frac{1}{k_B T} \cdot \frac{\delta F_r}{\delta \mathbf{p}}, \quad V_{Q_1} = \frac{1}{k_B T} \cdot \frac{\delta F_r}{\delta Q_1}, \quad V_{Q_2} = \frac{1}{k_B T} \cdot \frac{\delta F_r}{\delta Q_2}.$$

Direct computation gives

$$V_{\mathbf{p}} = c_{01}\mathbf{p} + c_{11}\nabla \cdot Q_1 + c_{12}\nabla \cdot Q_2 - c_{21}\Delta\mathbf{p} - c_{27}\nabla(\nabla \cdot \mathbf{p}), \quad (3.1)$$

$$V_{Q_1} = c_{02}Q_1 + c_{04}Q_2 - c_{11}\nabla\mathbf{p} - c_{22}\Delta Q_1 - c_{24}\Delta Q_2 - c_{28}\nabla(\nabla \cdot Q_1) - c_{2,10}\nabla(\nabla \cdot Q_2), \quad (3.2)$$

$$V_{Q_2} = c_{04}Q_1 + c_{03}Q_2 - c_{12}\nabla\mathbf{p} - c_{24}\Delta Q_1 - c_{23}\Delta Q_2 - c_{2,10}\nabla(\nabla \cdot Q_1) - c_{29}\nabla(\nabla \cdot Q_2). \quad (3.3)$$

And we can verify that

$$V = V_{\mathbf{p}} \cdot \mathbf{m}_1 + V_{Q_1} : \mathbf{m}_1 \mathbf{m}_1 + V_{Q_2} : \mathbf{m}_2 \mathbf{m}_2. \quad (3.4)$$

Thus

$$L_i V = V_{\mathbf{p}} \cdot (L_i \mathbf{m}_1) + V_{Q_1} : (L_i \mathbf{m}_1 \mathbf{m}_1) + V_{Q_2} : (L_i \mathbf{m}_2 \mathbf{m}_2). \quad (3.5)$$

From this equation, the elastic stress can be written as

$$\begin{aligned} \tau_e = & ck_B T \{ \langle \mathbf{m}_2 \mathbf{m}_2 - \mathbf{m}_3 \mathbf{m}_3 \rangle + V_{Q_2} : \langle (\mathbf{m}_2 \mathbf{m}_3 + \mathbf{m}_3 \mathbf{m}_2) \mathbf{m}_2 \mathbf{m}_3 \rangle \\ & + \langle \mathbf{m}_1 \mathbf{m}_1 - \mathbf{m}_3 \mathbf{m}_3 \rangle + V_{\mathbf{p}} \cdot \langle \mathbf{m}_3 \mathbf{m}_1 \mathbf{m}_3 \rangle + V_{Q_1} : \langle (\mathbf{m}_1 \mathbf{m}_3 + \mathbf{m}_3 \mathbf{m}_1) \mathbf{m}_1 \mathbf{m}_3 \rangle \\ & + \frac{1}{I_{11} + I_{22}} [(I_{22} - I_{11}) \langle \mathbf{m}_2 \mathbf{m}_2 - \mathbf{m}_1 \mathbf{m}_1 \rangle + V_{\mathbf{p}} \cdot \langle \mathbf{m}_2 (I_{22} \mathbf{m}_1 \mathbf{m}_2 - I_{11} \mathbf{m}_2 \mathbf{m}_1) \rangle \\ & + (V_{Q_1} - V_{Q_2}) : \langle (\mathbf{m}_1 \mathbf{m}_2 + \mathbf{m}_2 \mathbf{m}_1) (I_{22} \mathbf{m}_1 \mathbf{m}_2 - I_{11} \mathbf{m}_2 \mathbf{m}_1) \rangle] \}. \end{aligned} \quad (3.6)$$

And the external force is written as

$$\mathbf{F}_e = -ck_B T \nabla (V_{\mathbf{p}} \cdot \mathbf{p} + V_{Q_1} : Q_1 + V_{Q_2} : Q_2). \quad (3.7)$$

Now the equation (2.26) is only relevant to the tensors. For the equation (2.24), we multiply it by the tensors and integrate in SO_3 . Generally, we can write

$$\frac{\partial A}{\partial t} + \mathbf{v} \cdot \nabla A = \mathcal{N}_A + \mathcal{M}_A + \mathcal{V}_A, \quad (3.8)$$

where A is arbitrary tensor, and \mathcal{N}_A , \mathcal{M}_A , \mathcal{V}_A are the terms computed from spatial diffusion terms, rotational diffusion terms, and rotational convection terms. We need the integration by

parts (2.9) and (2.8) when computing these terms. Take Q_1 as an example. After multiplying $\mathbf{m}_1\mathbf{m}_1$ and doing the integration, the following term appears,

$$\begin{aligned}\int d\nu \mathbf{m}_1\mathbf{m}_1 D_2 L_2^2 f &= D_2 \int d\nu L_2^2(\mathbf{m}_1\mathbf{m}_1) f \\ &= D_2 \int d\nu 2(\mathbf{m}_3\mathbf{m}_3 - \mathbf{m}_1\mathbf{m}_1) f = 2D_2 \langle \mathbf{m}_3\mathbf{m}_3 - \mathbf{m}_1\mathbf{m}_1 \rangle.\end{aligned}\quad (3.9)$$

Similarly, we can derive that

$$\begin{aligned}-\mathcal{M}_{\mathbf{p}} &= D_2 [\mathbf{p} + V_{\mathbf{p}} \cdot \langle \mathbf{m}_3\mathbf{m}_3 \rangle + V_{Q_1} : (\langle \mathbf{m}_1\mathbf{m}_3\mathbf{m}_3 \rangle + \langle \mathbf{m}_3\mathbf{m}_1\mathbf{m}_3 \rangle)] \\ &\quad + D_3 [\mathbf{p} + V_{\mathbf{p}} \cdot \langle \mathbf{m}_2\mathbf{m}_2 \rangle + (V_{Q_1} - V_{Q_2}) : (\langle \mathbf{m}_1\mathbf{m}_2\mathbf{m}_2 \rangle + \langle \mathbf{m}_2\mathbf{m}_1\mathbf{m}_2 \rangle)].\end{aligned}\quad (3.10)$$

$$\begin{aligned}-\mathcal{M}_{Q_1} &= D_2 [2(Q_1 - Q_3) + V_{\mathbf{p}} \cdot (\langle \mathbf{m}_3\mathbf{m}_3\mathbf{m}_1 \rangle + \langle \mathbf{m}_3\mathbf{m}_1\mathbf{m}_3 \rangle)] \\ &\quad + V_{Q_1} : (\langle (\mathbf{m}_1\mathbf{m}_3 + \mathbf{m}_3\mathbf{m}_1)(\mathbf{m}_1\mathbf{m}_3 + \mathbf{m}_3\mathbf{m}_1) \rangle) \\ &\quad + D_3 [2(Q_1 - Q_2) + V_{\mathbf{p}} \cdot (\langle \mathbf{m}_2\mathbf{m}_2\mathbf{m}_1 \rangle + \langle \mathbf{m}_2\mathbf{m}_1\mathbf{m}_2 \rangle)] \\ &\quad + (V_{Q_1} - V_{Q_2}) : (\langle (\mathbf{m}_1\mathbf{m}_2 + \mathbf{m}_2\mathbf{m}_1)(\mathbf{m}_1\mathbf{m}_2 + \mathbf{m}_2\mathbf{m}_1) \rangle)].\end{aligned}\quad (3.11)$$

$$\begin{aligned}-\mathcal{M}_{Q_2} &= D_1 [2(Q_2 - Q_3) + V_{Q_2} : (\langle (\mathbf{m}_2\mathbf{m}_3 + \mathbf{m}_3\mathbf{m}_2)(\mathbf{m}_2\mathbf{m}_3 + \mathbf{m}_3\mathbf{m}_2) \rangle)] \\ &\quad + D_3 [2(Q_2 - Q_1) - V_{\mathbf{p}} \cdot (\langle \mathbf{m}_2\mathbf{m}_2\mathbf{m}_1 \rangle + \langle \mathbf{m}_2\mathbf{m}_1\mathbf{m}_2 \rangle)] \\ &\quad - (V_{Q_1} - V_{Q_2}) : (\langle (\mathbf{m}_1\mathbf{m}_2 + \mathbf{m}_2\mathbf{m}_1)(\mathbf{m}_1\mathbf{m}_2 + \mathbf{m}_2\mathbf{m}_1) \rangle)].\end{aligned}\quad (3.12)$$

$$\mathcal{V}_{\mathbf{p}} = \kappa : \left[\langle \mathbf{m}_1\mathbf{m}_3\mathbf{m}_3 \rangle + \frac{I_{22}}{I_{11} + I_{22}} \langle \mathbf{m}_1\mathbf{m}_2\mathbf{m}_2 \rangle - \frac{I_{11}}{I_{11} + I_{22}} \langle \mathbf{m}_2\mathbf{m}_1\mathbf{m}_2 \rangle \right].\quad (3.13)$$

$$\begin{aligned}\mathcal{V}_{Q_1} &= \kappa : \left[\langle \mathbf{m}_1\mathbf{m}_3(\mathbf{m}_1\mathbf{m}_3 + \mathbf{m}_3\mathbf{m}_1) \rangle + \frac{I_{22}}{I_{11} + I_{22}} \langle \mathbf{m}_1\mathbf{m}_2(\mathbf{m}_1\mathbf{m}_2 + \mathbf{m}_2\mathbf{m}_1) \rangle \right. \\ &\quad \left. - \frac{I_{11}}{I_{11} + I_{22}} \langle \mathbf{m}_2\mathbf{m}_1(\mathbf{m}_1\mathbf{m}_2 + \mathbf{m}_2\mathbf{m}_1) \rangle \right].\end{aligned}\quad (3.14)$$

$$\begin{aligned}\mathcal{V}_{Q_2} &= \kappa : \left[\langle \mathbf{m}_2\mathbf{m}_3(\mathbf{m}_2\mathbf{m}_3 + \mathbf{m}_3\mathbf{m}_2) \rangle - \frac{I_{22}}{I_{11} + I_{22}} \langle \mathbf{m}_1\mathbf{m}_2(\mathbf{m}_1\mathbf{m}_2 + \mathbf{m}_2\mathbf{m}_1) \rangle \right. \\ &\quad \left. + \frac{I_{11}}{I_{11} + I_{22}} \langle \mathbf{m}_2\mathbf{m}_1(\mathbf{m}_1\mathbf{m}_2 + \mathbf{m}_2\mathbf{m}_1) \rangle \right].\end{aligned}\quad (3.15)$$

$$\begin{aligned}(\mathcal{N}_{\mathbf{p}})_{\alpha} &= \partial_i \left(\partial_j \sum_{\sigma=1}^3 \gamma_{\sigma} \langle m_{1\alpha} m_{\sigma i} m_{\sigma j} \rangle + \partial_j (V_{\mathbf{p}})_k \sum_{\sigma=1}^3 \gamma_{\sigma} \langle m_{1k} m_{1\alpha} m_{\sigma i} m_{\sigma j} \rangle \right. \\ &\quad + \partial_j (V_{Q_1})_{kl} \sum_{\sigma=1}^3 \gamma_{\sigma} \langle m_{1k} m_{1l} m_{1\alpha} m_{\sigma i} m_{\sigma j} \rangle \\ &\quad \left. + \partial_j (V_{Q_2})_{kl} \sum_{\sigma=1}^3 \gamma_{\sigma} \langle m_{2k} m_{2l} m_{1\alpha} m_{\sigma i} m_{\sigma j} \rangle \right).\end{aligned}\quad (3.16)$$

$$\begin{aligned}(\mathcal{N}_{Q_1})_{\alpha\beta} &= \partial_i \left(\partial_j \sum_{\sigma=1}^3 \gamma_{\sigma} \langle m_{1\alpha} m_{1\beta} m_{\sigma i} m_{\sigma j} \rangle + \partial_j (V_{\mathbf{p}})_k \sum_{\sigma=1}^3 \gamma_{\sigma} \langle m_{1k} m_{1\alpha} m_{1\beta} m_{\sigma i} m_{\sigma j} \rangle \right. \\ &\quad + \partial_j (V_{Q_1})_{kl} \sum_{\sigma=1}^3 \gamma_{\sigma} \langle m_{1k} m_{1l} m_{1\alpha} m_{1\beta} m_{\sigma i} m_{\sigma j} \rangle \\ &\quad \left. + \partial_j (V_{Q_2})_{kl} \sum_{\sigma=1}^3 \gamma_{\sigma} \langle m_{2k} m_{2l} m_{1\alpha} m_{1\beta} m_{\sigma i} m_{\sigma j} \rangle \right).\end{aligned}\quad (3.17)$$

$$\begin{aligned}
(\mathcal{N}_{Q_2})_{\alpha\beta} = & \partial_i \left(\partial_j \sum_{\sigma=1}^3 \gamma_\sigma \langle m_{2\alpha} m_{2\beta} m_{\sigma i} m_{\sigma j} \rangle + \partial_j (V_{\mathbf{p}})_k \sum_{\sigma=1}^3 \gamma_\sigma \langle m_{1k} m_{2\alpha} m_{2\beta} m_{\sigma i} m_{\sigma j} \rangle \right. \\
& + \partial_j (V_{Q_1})_{kl} \sum_{\sigma=1}^3 \gamma_\sigma \langle m_{1k} m_{1l} m_{2\alpha} m_{2\beta} m_{\sigma i} m_{\sigma j} \rangle \\
& \left. + \partial_j (V_{Q_2})_{kl} \sum_{\sigma=1}^3 \gamma_\sigma \langle m_{2k} m_{2l} m_{2\alpha} m_{2\beta} m_{\sigma i} m_{\sigma j} \rangle \right). \tag{3.18}
\end{aligned}$$

To make the equations form a closed system, we need to express high-order tensors as functions of (\mathbf{p}, Q_1, Q_2) . Here we use the quasi-equilibrium approximation, namely to choose f that minimizes the entropy term $\int d\nu f \log f$ with (\mathbf{p}, Q_1, Q_2) equal to the given value. Remember that $f = c\rho$ where c is constant. Thus ρ is given by [38]

$$\rho(P) = \frac{1}{Z} \exp(\mathbf{b} \cdot \mathbf{m}_1 + B_1 : \mathbf{m}_1 \mathbf{m}_1 + B_2 : \mathbf{m}_2 \mathbf{m}_2), \tag{3.19}$$

where \mathbf{b} is a vector, B_1 and B_2 are symmetric matrices, and

$$Z = \int d\nu \exp(\mathbf{b} \cdot \mathbf{m}_1 + B_1 : \mathbf{m}_1 \mathbf{m}_1 + B_2 : \mathbf{m}_2 \mathbf{m}_2). \tag{3.20}$$

Now the system is described by (\mathbf{p}, Q_1, Q_2) . The evolution of three tensors is governed by (3.8) in which the terms are given by (3.10)-(3.18), together with (2.25) and (2.26) in which the terms are given by (2.36), (3.6), (3.7). The high-order tensors are computed from (3.19), which keeps f positive and the energy dissipation law. It is obvious that f is positive, and we can deduce that

$$\begin{aligned}
& \frac{d}{dt} \left(F[\mathbf{p}, Q_1, Q_2] + \int d\mathbf{x} \frac{\rho |\mathbf{v}|^2}{2} \right) \\
= & \int d\mathbf{x} \left\{ -ck_B T [D_1 \langle (\mu_{Q_2} : (\mathbf{m}_2 \mathbf{m}_3 + \mathbf{m}_3 \mathbf{m}_2))^2 \rangle \right. \\
& + D_2 \langle (\mu_{\mathbf{p}} \cdot \mathbf{m}_3 + \mu_{Q_1} : (\mathbf{m}_2 \mathbf{m}_3 + \mathbf{m}_3 \mathbf{m}_2))^2 \rangle \\
& + D_3 \langle (\mu_{\mathbf{p}} \cdot \mathbf{m}_2 + (\mu_{Q_1} - \mu_{Q_2}) : (\mathbf{m}_2 \mathbf{m}_3 + \mathbf{m}_3 \mathbf{m}_2))^2 \rangle] \\
& - ck_B T \sum_{\sigma=1}^3 \gamma_\sigma \langle [\partial_j (\mu_{\mathbf{p}})_k m_{1k} m_{\sigma j} + \partial_j (\mu_{Q_1})_{kl} m_{1k} m_{1l} m_{\sigma j} + \partial_j (\mu_{Q_2})_{kl} m_{2k} m_{2l} m_{\sigma j}]^2 \rangle \\
& - 2\eta \frac{\kappa + \kappa^T}{2} : \frac{\kappa + \kappa^T}{2} - c\zeta \left[I_{22} \langle (\kappa : \mathbf{m}_1 \mathbf{m}_1)^2 \rangle + I_{11} \langle (\kappa : \mathbf{m}_2 \mathbf{m}_2)^2 \rangle \right. \\
& \left. + \frac{I_{11} I_{22}}{I_{11} + I_{22}} \langle (\kappa : (\mathbf{m}_1 \mathbf{m}_2 + \mathbf{m}_2 \mathbf{m}_1))^2 \rangle \right] \left. \right\}. \tag{3.21}
\end{aligned}$$

In the above, we denote $\mu_{\mathbf{p}} = \delta F / \delta \mathbf{p}$, etc. The details are given in Appendix. Note that each of the right-hand terms is not positive.

4 Numerical results

In this section, we focus on the shear flow problem. We assume that the velocity is along the x -direction, and the gradient is along the y -direction, and

$$\kappa_{12} = \partial_2 v_1 = k$$

is a constant. We also assume that the tensors are spatially homogeneous. Thus, we only need the bulk energy in (2.42) and will discard the gradient terms. In this case, the equation of momentum holds naturally, and we need to solve the Smoluchowski equation only.

We rescale the time unit by $\tilde{t} = (\zeta l^2 / 48 k_B T)^{-1} t$. It cancels the $k_B T$ in the free energy and the units in the rotational diffusion coefficients D_i . For bent-core molecules, the rescaling let

$$(D_1^{-1}, D_2^{-1}, D_3^{-1}) = (4 \sin^2 \frac{\theta}{2}, \cos^2 \frac{\theta}{2}, 1 + 3 \sin^2 \frac{\theta}{2}).$$

After the rescaling, the shear rate k becomes dimensionless. In the free energy, by (2.43) we rescale $\tilde{\mathbf{x}} = \mathbf{x}/l$ and reduce the shape parameters to three dimensionless ones: $\eta = D/l$, l_2/l , and θ . We fix $\eta = 1/40$, and express the concentration by $\alpha = cD^2(l+l_2)$ that is proportional to the volume fraction $(\pi/4)cD^2(l+l_2)$.

In what follows, we examine both the molecular model and the tensor model, and compare the flowing modes shown by both models.

4.1 Numerical method

For the tensor model, we use (3.19) to convert the equations of tensors into equations of (\mathbf{b}, B_1, B_2) ,

$$\frac{d(\mathbf{b}, B_1, B_2)}{dt} = \left(\frac{\partial(\mathbf{p}, Q_1, Q_2)}{\partial(\mathbf{b}, B_1, B_2)} \right)^{-1} \frac{d(\mathbf{p}, Q_1, Q_2)}{dt}. \quad (4.1)$$

The derivatives $\frac{\partial(\mathbf{p}, Q_1, Q_2)}{\partial(\mathbf{b}, B_1, B_2)}$ are computed by (A.4). They are expressed by high-order tensors. The tensors are computed by numerical integration about the Euler angles. Each of the Euler angles are discretized by 32 points. The time discretization is implemented by the classical fourth-order Runge-Kutta method with the time step $\delta t = 10^{-2}$. The initial value is chosen as $B_1 = B_2 = 0$, while $\mathbf{b} = (1.4, 2.8, 1.4)^T$ pointing to a tilted direction.

For the molecular model, we adopt a spectral-Galerkin method, where we use Wigner D-matrix $D_{mm'}^j$ (see, for example, [37]), truncated at $j \leq 10$, to discretize the density function f . For the time integration, we also use the classical fourth-order Runge-Kutta method, with the time step $\delta t = 5 \times 10^{-3}$. For the initial value, we start from the Boltzmann distribution with $B_1 = B_2 = 0$ and $\mathbf{b} = (1.4, 2.8, 1.4)^T$. We let it evolve 2000 time steps under the parameter $\alpha = 0.5$, $\theta = 23\pi/32$, $k = 6.4$, and take the result as the initial value.

4.2 Flow modes

Before looking at the flow modes, we review the homogeneous nematic phases shown by bent-core molecules and star molecules in quiescent fluid, namely $k = 0$, which are discussed in [38]. In these phases we have $\mathbf{p} = 0$. Denote $Q_3 = \langle \mathbf{m}_3 \mathbf{m}_3 \rangle = I - Q_1 - Q_2$. Bent-core molecules and star molecules can exhibit the uniaxial nematic phase, where we can find a unit vector \mathbf{n} such that

$$Q_i = s_i(\mathbf{n}\mathbf{n} - \frac{I}{3}) + \frac{I}{3}, \quad i = 1, 2, 3.$$

According to the signs of s_i , the uniaxial nematic phase is further classified. It is the N_2 phase where $s_1, s_3 < 0$, $s_2 > 0$, indicating that \mathbf{m}_2 accumulates near \mathbf{n} and $\mathbf{m}_1, \mathbf{m}_3$ accumulate near the plane vertical to \mathbf{n} ; and the N_3 phase where $s_1, s_2 < 0$, $s_3 > 0$, indicating that

\mathbf{m}_3 accumulates near \mathbf{n} and $\mathbf{m}_2, \mathbf{m}_3$ accumulate near the plane vertical to \mathbf{n} . We can also observe the biaxial nematic phase (B), where we can find an orthonormal frame $(\mathbf{n}_1, \mathbf{n}_2, \mathbf{n}_3)$ such that

$$Q_i = s_{i1}\mathbf{n}_1\mathbf{n}_1 + s_{i2}\mathbf{n}_2\mathbf{n}_2 + s_{i3}\mathbf{n}_3\mathbf{n}_3.$$

The eigenvalues satisfy $s_{ii} > s_{ij}$ ($j \neq i$), indicating that \mathbf{m}_i is preferably along \mathbf{n}_i .

Both bent-core molecules and star molecules exhibit the isotropic phase with small α , and the modulated twist-bend phase with large α . Thus, in this work we will choose intermediate α to let the system have homogeneous nematic phases in equilibrium. For bent-core molecules, we choose $\alpha = 0.42, 0.5$, and examine the bending angles $\theta = j\pi/32$ where $16 \leq j \leq 23$. For both α , it shows the N_2 phase for $20 \leq j \leq 23$, the N_3 phase for $16 \leq j \leq 18$, and the B phase for $j = 19$. For star molecules, we fix $\alpha = 0.42$, $\theta = 2\pi/3$ and examine $l_2/l = j/40$ where $5 \leq j \leq 11$. It shows the N_2 phase when $j = 5$, the N_3 phase when $j = 11$, and the B phase when $6 \leq j \leq 10$.

We choose the shear rates as $k = 0.2n$, $n = 1, \dots, 100$. Since \mathbf{p} is zero in quiescent fluid, we are interested in whether \mathbf{p} appears. Actually, under our choice of parameters, $|\mathbf{p}|$ always decays rapidly. This should be the result of $c_{01} > 0$ (see [39]). In the following, we no longer look at \mathbf{p} and focus on Q_1 and Q_2 . Denote the unit eigenvector of the largest eigenvalue of Q_i as \mathbf{q}_i for $i = 1, 2$. Note that in quiescent fluid \mathbf{q}_1 and \mathbf{q}_2 are vertical. Although it does not hold in shear flow, we find that \mathbf{q}_1 and \mathbf{q}_2 are always approximately vertical. Actually, in most cases, we have $\cos\langle\mathbf{q}_1, \mathbf{q}_2\rangle \leq 0.1$. This value may become a little larger when the shear rate k is near the transition value between two flow modes. At that time, the largest and second eigenvalues of Q_1 or Q_2 might be very close so that \mathbf{q}_1 and \mathbf{q}_2 are sensitive to the value of Q_1 and Q_2 . Thus, we may view the molecule as having a preferred orientation such that \mathbf{m}_i is near \mathbf{q}_i , and classify the flow modes according to the motion of \mathbf{q}_i .

4.2.1 Molecular model

For the molecular model, the flow modes are described below.

1. Log-rolling (LR): steady state, where \mathbf{q}_2 is along the z - (vortex) direction, and \mathbf{q}_1 lies in the x - y (shear) plane.
2. Kayaking(K): one of \mathbf{q}_1 and \mathbf{q}_2 rotates round the z -axis, while the other shows a splayed pattern (see Fig. 4 left). If \mathbf{q}_i rotates round the z -axis, we denote the flow mode as K- Q_i .
3. Double splayed (DS): \mathbf{q}_2 shows splayed pattern near the x -axis, \mathbf{q}_1 shows splayed near the y -axis (see Fig. 4 right).
4. Tumbling (T): \mathbf{q}_2 rotates in the x - y plane; \mathbf{q}_1 also rotates in the plane, but jumps to z when it approaches the y axis (see Fig. 3 left).
5. Wagging: \mathbf{q}_2 shows wagging near the x -axis. According to the motion of \mathbf{q}_1 , it is further classified into two cases.
 - Wagging-alternating (W-A): \mathbf{q}_1 is wagging near the y -axis, with a jump to the z -axis (see Fig. 3 right).
 - Wagging-wagging (W-W): \mathbf{q}_1 is wagging near the y -axis.

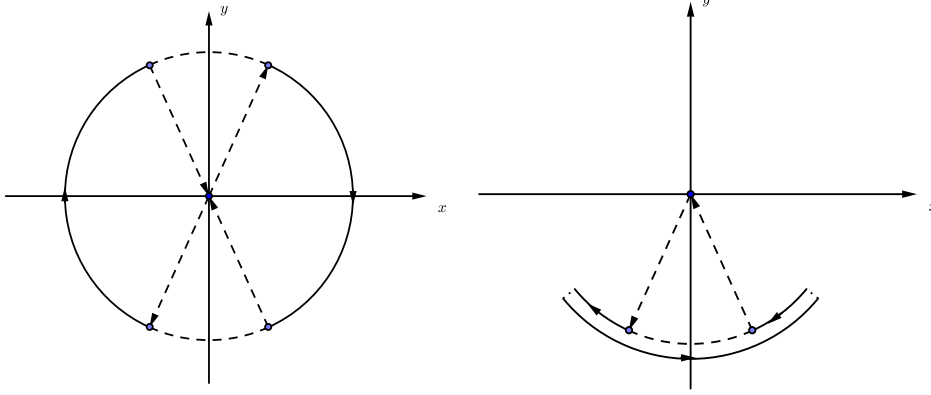


Fig. 3: Left: Tumbling motion of \mathbf{q}_1 . Right: Wagging-alternating motion of \mathbf{q}_1 .

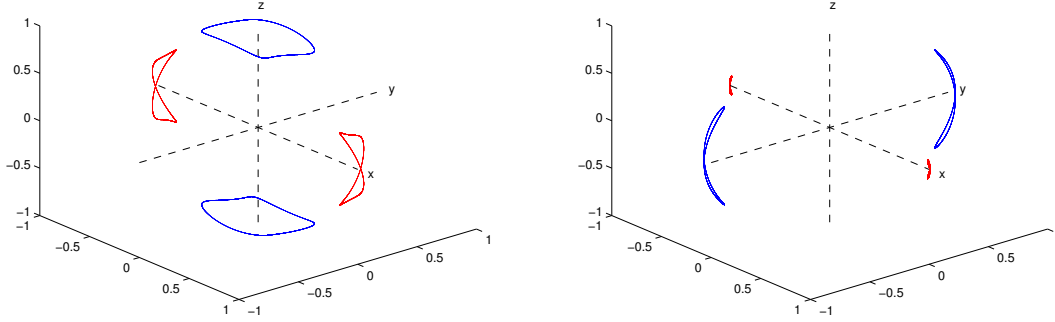


Fig. 4: Left: Kayaking. The red and blue lines are motions of $\pm\mathbf{q}_1$ and $\pm\mathbf{q}_2$: when \mathbf{q}_1 corresponds to blue line, it shows K- Q_1 mode; otherwise it shows K- Q_2 mode. Right: Double splayed, where red line gives the motion of $\pm\mathbf{q}_2$, and blue line gives the motions of $\pm\mathbf{q}_1$.

6. Flow-aligning (FA): steady state, where \mathbf{q}_2 lies in the x - y plane, while \mathbf{q}_1 may be in the x - y plane (FA- y) or along the z axis (FA- z).

First we examine the flow modes for bent-core molecules. The range of shear rates for each flow mode in molecular model is listed in Table 1a and Table 1b. For $\theta = 19\pi/32$ and $\alpha = 0.5$, the flow modes are

$$\text{K-}Q_2 : [0, 2.8], \quad \text{K-}Q_1 : [3.0, 6.8], \quad \text{FA-}z : [7.0, 20.0].$$

We have mentioned that in quiescent fluid, the bending angle $\theta = j\pi/32$ determines which of the three nematic phase is observed. In shear flow, different nematic phases result in distinct flow mode sequences with the shear rate k increasing. When $16 \leq j \leq 18$, namely the equilibrium phase is N_3 , the only flow mode is FA- z . When $j = 19$, namely the equilibrium phase is B , we obtain only FA- z for $\alpha = 0.42$, and the K- Q_2 — K- Q_1 — FA- z sequence for $\alpha = 0.5$. When $20 \leq j \leq 23$, namely the equilibrium phase is N_2 , the sequence follows LR — K- Q_2 — T — W-A — W-W — FA- y — FA- z , with one or two modes missing. For $\alpha = 0.42$,

θ	LR	K- Q_2	T	W-A	W-W	FA- y	FA- z
$23\pi/32$	-	[0, 10.0]	[10.2, 12.0]	[12.2, 14.8]	[15.0, 17.0]	[17.2, 20.0]	-
$22\pi/32$	[0.2, 7.0]	[7.2, 8.6]	[8.8, 9.4]	[9.6, 12.0]	[12.2, 13.6]	[13.8, 20.0]	-
$21\pi/32$	[0.2, 5.6]	-	[5.8, 6.0]	[6.2, 8.0]	[8.2, 9.6]	[9.8, 16.2]	[16.4, 20.0]
$20\pi/32$	[0.2, 2.8]	[3.0, 3.4]	-	-	[3.6, 5.2]	[5.4, 11.0]	[11.2, 20.0]
$18\pi/32$	-	-	-	-	-	-	[0.2, 20.0]
$17\pi/32$	-	-	-	-	-	-	[0.2, 20.0]
$16\pi/32$	-	-	-	-	-	-	[0.2, 20.0]

(a) $\alpha = 0.5$.

θ	LR	K- Q_2	T	W-A	W-W	FA- y	FA- z
$23\pi/32$	[0.2, 9.0]	[9.2, 9.4]	-	[9.6, 11.0]	[11.2, 12.0]	[12.2, 18.6]	[18.8, 20.0]
$22\pi/32$	[0.2, 6.2]	6.4	-	[6.6, 8.4]	[8.6, 9.2]	[9.4, 14.6]	[14.8, 20.0]
$21\pi/32$	[0.2, 3.4]	3.6	-	[3.8, 4.8]	[5.0, 5.8]	[6.0, 10.2]	[10.4, 20.0]
$20\pi/32$	-	[0.2, 1.4]	-	[1.6, 2.0]	[2.2, 2.6]	[2.8, 6.0]	[6.2, 20.0]
$19\pi/32$	-	-	-	-	-	-	[0.2, 20.0]
$18\pi/32$	-	-	-	-	-	-	[0.2, 20.0]
$17\pi/32$	-	-	-	-	-	-	[0.2, 20.0]
$16\pi/32$	-	-	-	-	-	-	[0.2, 20.0]

(b) $\alpha = 0.42$.Table 1: Range of the shear rate k for flow modes in the molecular model for bent-core molecules.

T is missing for all the four angles, and LR is not shown for $j = 20$. For $\alpha = 0.5$, LR is not found for $j = 23$, K- Q_2 is not shown for $j = 21$, T and W-A are missing for $j = 20$, and FA- z is not exhibited for $j = 22, 23$.

For star molecules, we can have a closer look at the effect of molecular shape in the biaxial region. As l_2/l increases, the equilibrium phase sequence is $N_2 - B - N_3$. At $l_2/l = 0.125$, the flow mode sequence is LR - K- Q_2 - W-W - FA- y - FA- z , which is part of the sequence found for bent-core molecules in the N_2 region. When l_2/l increases and enters the B region, the K- Q_1 mode emerges between FA- y and FA- z . Then we observe some subtle phenomena when l_2/l further increases. At $l_2/l = 0.2$, the K- Q_2 mode moves to the middle of FA- y and K- Q_1 . At $l_2/l = 0.225$, the mode at low shear rates changes from LR to K- Q_2 and LR emerges at high shear rates, resulting in the sequence K- Q_2 - W-W - FA- y - K- Q_2 -

l_2/l	LR	K- Q_2	W-W	DS	FA- y	K- Q_1	FA- z
0.125	[0.2, 4.4]	[4.6, 5.2]	[5.4, 6.8]	-	[7.0, 11.8]	-	[12.0, 20.0]
0.15	[0.2, 4.2]	[4.4, 5.0]	[5.2, 6.2]	-	[6.4, 11.0]	[11.2, 12.8]	[13.0, 20.0]
0.175	[0.2, 3.8]	[4.0, 4.4]	[4.6, 4.8]	-	[5.0, 10.4]	[10.6, 12.4]	[12.6, 20.0]
0.2	[0.2, 3.0]	[10.0, 10.6]	[3.2, 4.4]	-	[4.6, 9.8]	[10.8, 11.2]	[11.4, 20.0]
0.225	[9.8, 11.6]	[0.2, 1.8], [9.2, 9.6]	[2.0, 3.0]	-	[3.2, 9.0]	-	[11.8, 20.0]
0.25	[8.8, 12.6]	[0.2, 1.0]	[1.2, 1.8]	-	[2.0, 8.6]	-	[12.8, 20.0]
0.275	[8.4, 13.4]	-	-	[0.2, 2.4]	[2.6, 8.2]	-	[13.6, 20.0]

Table 2: Range of the shear rate k for flow modes in the molecular model for star molecules, $\alpha = 0.42$.

LR — FA- z . Then at $l_2/l = 0.25$, K- Q_2 at high shear rates vanishes. Finally at $l_2/l = 0.275$, the two periodic modes K- Q_2 and W-W are substituted by DS.

Because rod-like molecules also show the N_2 phase in equilibrium, we would like to compare the flow modes of bent-core molecules with $\theta = j\pi/32$, $20 \leq j \leq 23$ with those of rod-like molecules that have been studied extensively in literature. If we only look at the motion of \mathbf{q}_2 , the five modes are also found for rod-like molecules. The out-of-plane steady and out-of-plane oscillating states are also exhibited by rod-like molecules but are not shown in our results. The works on rod-like molecules imply that the occurrence of two out-of-plane modes might require a careful choice of α near the isotropic-nematic transition (see the solution diagrams in [12]). Our choice of α , however, is significantly larger than the transition value.

4.2.2 Tensor model

We only examine the bent-core molecules using the tensor model. The range of shear rates for each flow mode in tensor models is listed in Table 3a and Table 3b. For $\theta = 19\pi/32$ and $\alpha = 0.5$, the flow modes are

$$\text{DS} : [0, 8.4], \quad \text{K-}Q_1 : [8.6, 16.8], \quad \text{FA-}z : [17.0, 20.0].$$

We compare the results of tensor model with molecular model. Although under different shape parameters, we can observe all the flow modes found in the molecular model. For $16 \leq j \leq 18$, the only mode FA- z is the same as molecular model. This is also the case for $j = 19$ and $\alpha = 0.42$. For $j = 19$ and $\alpha = 0.5$, the DS takes the place of K- Q_2 , while the K- Q_1 and FA- z coincide with the molecular model. For $j = 20$, the sequence in the tensor model covers that in the molecular model, with the extra LR for $\alpha = 0.42$ and W-A for $\alpha = 0.5$. For $21 \leq j \leq 23$, the tensor model captures only the modes occurring at lower shear rate in the molecular model. Specifically, we do not observe W-W, FA- y and FA- z for the three j , and W-A for $j = 23$ and $\alpha = 0.5$. Some missing modes in molecular model are exhibited, including T for $\alpha = 0.42$ and $j = 22, 23$, K- Q_2 for $\alpha = 0.5$ and $j = 21$, and LR for $\alpha = 0.5$ and $j = 23$.

For the rod-like molecules, the tensor model with Bingham closure has been examined and compared with the molecular model. The results (see [19, 40]) suggest that the tensor model works better when α is near the isotropic-nematic transition value, and at low shear rate. This is also observed in our results for bent-core molecules for $20 \leq j \leq 23$. Because the I-N transition value increases as θ decreases, the α we choose is nearer to the I-N transition value for $j = 20$ than $21 \leq j \leq 23$. Indeed, for $j = 20$, the flow mode sequence in tensor model better reflects that in molecular model.

4.3 Discussion

We compare our model and the results with those in [31], where simulation is done for a molecular model, namely a model of the density function f .

From the modeling viewpoint, the model in [31] has some limitations. It adopts a simple free energy, where the order parameters only include Q_1 and Q_2 , which are not complete to describe the symmetry of the bent-core molecules. Also, the elastic energy and the spatial diffusion are also not included. Since bent-core molecules are able to show modulated nematic phases (see [38]), the model in [31] is only appropriate for homogeneous flows. Our model

θ	LR	K- Q_2	T	W-A	W-W	FA- y	FA- z
$23\pi/32$	[0.2, 12.2]	[12.4, 19.2]	[19.4, 20.0]	-	-	-	-
$22\pi/32$	[0.2, 8.6]	[8.8, 13.0]	[13.2, 14.4]	[14.6, 20.0]	-	-	-
$21\pi/32$	[0.2, 4.8]	[5.0, 7.4]	[7.6, 8.6]	[8.8, 20.0]	-	-	-
$20\pi/32$	[0.2, 1.4]	[1.6, 3.0]	-	[3.2, 5.8]	[6.0, 14.6]	[14.8, 19.6]	[19.8, 20.0]
$18\pi/32$	-	-	-	-	-	-	[0.2, 20.0]
$17\pi/32$	-	-	-	-	-	-	[0.2, 20.0]
$16\pi/32$	-	-	-	-	-	-	[0.2, 20.0]

(a) $\alpha = 0.5$.

θ	LR	K- Q_2	T	W-A	W-W	FA- y	FA- z
$23\pi/32$	[0.2, 7.4]	[7.6, 10.4]	[10.6, 12.0]	[12.2, 20.0]	-	-	-
$22\pi/32$	[0.2, 4.4]	[4.6, 6.6]	[6.8, 7.4]	[7.6, 20.0]	-	-	-
$21\pi/32$	[0.2, 1.8]	[2.0, 3.4]	-	[3.6, 20.0]	-	-	-
$20\pi/32$	[0.2, 0.6]	[0.8, 1.0]	-	[1.2, 1.8]	[2.0, 7.4]	[7.6, 10.4]	[10.6, 20.0]
$19\pi/32$	-	-	-	-	-	-	[0.2, 20.0]
$18\pi/32$	-	-	-	-	-	-	[0.2, 20.0]
$17\pi/32$	-	-	-	-	-	-	[0.2, 20.0]
$16\pi/32$	-	-	-	-	-	-	[0.2, 20.0]

(b) $\alpha = 0.42$.Table 3: Range of the shear rate k for flow modes in the tensor model for bent-core molecules.

takes the above three aspects into account, which enables us to study inhomogeneous flows in the future.

Another thing we would like to point out is that [31] derives the terms in the model using distinct molecular architectures, as stated in that work. This leads to different expressions from what we obtain of the rotational diffusion coefficients, the rotational convection, and the stress tensor. Usually this approach can be a good approximation, but is insufficient if we aim to investigate the effect of molecular architecture. Moreover, we note that the coefficients of the bulk free energy are different. The difference in coefficients may lead to different phase behavior, thus may cause significant distinction in flow modes, which is indeed reflected in our results.

We observe some similar results in our simulation and in [31]. We confirm that $\mathbf{p} = 0$, validating the choice of bulk energy without \mathbf{p} in the homogeneous case. Also, the occurrence of LR phase at low shear rate and FA phase at high shear rate is identical. However, the periodic flow modes are different, which can be expected because there are many differences in the terms and coefficients. Our model shows some flow modes analogous to those of rod-like molecules, while [31] reported some modes where the motion of \mathbf{q}_i are tilted.

Finally, we discuss the mixed moments $\langle \mathbf{m}_i \mathbf{m}_j \rangle$, ($i \neq j$). In our model, they are zero in both molecular and tensor model, which is consistent with the molecular symmetry. We can also prove it directly from the dynamic model. Actually, in the tensor model, from the Boltzmann distribution, $\langle \mathbf{m}_i \mathbf{m}_j \rangle = 0$ for $i \neq j$. Also, in the molecular model, if the equality

$$f(P(\alpha, \beta, \gamma), t) = f(P(\alpha, \beta, \gamma + \pi), t) = f(P(\pi - \alpha, \beta + \pi, \pi - \gamma), t) = f(P(\pi - \alpha, \beta, -\gamma), t)$$

holds for $t = 0$, we can prove that it holds for arbitrary $t > 0$ (see Appendix). We then derive from the above symmetric property that $\langle \mathbf{m}_i \mathbf{m}_j \rangle = 0$ for $i \neq j$.

5 Conclusion

In this work, we establish the molecular model and tensor model for the dynamics of bent-core molecules and star molecules in incompressible fluid. We assume that the molecule is rigid consisting of spheres. Based on this architecture, we build hardcore molecular interaction and sphere–fluid friction into the model. In this way, we obtain the molecular model fully determined by physical parameters, which clearly reflects the molecular shape in the model. The molecular model incorporates three tensors describing polar and biaxial order, elastic energy that is able to describe the modulation, convection and diffusion both spatially and orientationally, and the corresponding stress and external force that let the system be energy dissipative. The tensor model is then derived from the molecular model. Along with the quasi-equilibrium closure approximation, the tensor model is also energy dissipative.

We use both molecular model and tensor model to examine the flow modes in the shear flow problem. We focus on the effect of bending angle of bent-core molecules, and the length of the extra arm of star molecules. The parameters are chosen to cover the transition between three nematic phases N_2 , B and N_3 . We examine the change of flow modes when the parameters go across the $N_2 - B$ and $B - N_3$ phase boundaries. When the equilibrium phase is N_2 , we find the flow modes analogous to the rod-like molecules. The tensor model is able to capture all the flow modes shown by the molecular model. Under our choice of parameters, the flow mode sequence is mostly identical to that in the molecular model for smaller bending angles, and recovers the part of sequence in the molecular model at low shear rate for larger bending angles.

Although we only examined the shear flow problem, both the molecular model and the tensor model are ready for the studies of inhomogeneous flows. Also, for the shear flow problem, the model can be applied to other molecules with the same symmetry to carry out extensive investigations of the effect of molecular shape. The efficient implementation of closure approximation is also worth discussion. Currently we compute the quasi-equilibrium approximation by integration, which is time-consuming. Besides, the formulation of the tensor model allows us to adopt simpler closure approximations that might be suitable for specific types of flows, which is expected to be done in the future.

A Some equalities about the closure

Suppose f is given by (3.19), and Z is defined in (3.20). Direct computation gives

$$\frac{F_{entropy}}{k_B T} = \int d\nu \rho(\mathbf{x}, P) \log \rho(\mathbf{x}, P) = \mathbf{b} \cdot \mathbf{p} + B_1 : Q_1 + B_2 : Q_2 - \log Z, \quad (\text{A.1})$$

and

$$\frac{\partial \log Z}{\partial(\mathbf{b}, B_1, B_2)} = \frac{1}{Z} \frac{\partial Z}{\partial(\mathbf{b}, B_1, B_2)} = (\mathbf{p}, Q_1, Q_2). \quad (\text{A.2})$$

Thus we can deduce that (see [38])

$$\frac{1}{k_B T} \frac{\partial F_{entropy}}{\partial(\mathbf{p}, Q_1, Q_2)} = (\mathbf{b}, B_1, B_2). \quad (\text{A.3})$$

Moreover, The Jacobian $\frac{\partial(\mathbf{p}, Q_1, Q_2)}{\partial(\mathbf{b}, B_1, B_2)}$ can be expressed by high-order tensors,

$$\begin{aligned}\frac{\partial(\mathbf{p}, Q_1, Q_2)}{\partial(\mathbf{b}, B_1, B_2)} &= \frac{\partial^2 \log Z}{\partial(\mathbf{b}, B_1, B_2)^2} \\ &= \langle (\mathbf{m}_1, \mathbf{m}_1 \mathbf{m}_1, \mathbf{m}_2 \mathbf{m}_2) (\mathbf{m}_1, \mathbf{m}_1 \mathbf{m}_1, \mathbf{m}_2 \mathbf{m}_2) \rangle - (\mathbf{p}, Q_1, Q_2) (\mathbf{p}, Q_1, Q_2) \\ &= \text{cov}(\mathbf{m}_1, \mathbf{m}_1 \mathbf{m}_1, \mathbf{m}_2 \mathbf{m}_2).\end{aligned}\tag{A.4}$$

B The proof of the energy dissipation law of the tensor model

Now we prove the energy dissipation law, for which we need to rewrite the diffusion terms. From (A.3), we can write

$$\mu = k_B T + \mu_{\mathbf{p}} \cdot \mathbf{m}_1 + \mu_{Q_1} : \mathbf{m}_1 \mathbf{m}_1 + \mu_{Q_2} : \mathbf{m}_2 \mathbf{m}_2.\tag{B.1}$$

Here we denote $\mu_{\mathbf{p}} = \delta F / \delta \mathbf{p}$ etc., and F is the free energy. Thus the terms like (3.9) are rewritten as

$$\begin{aligned}& - \int d\nu \mathbf{m}_1 \mathbf{m}_1 D_2 L_2^2 f = D_2 \int d\nu f L_2(\mathbf{m}_1 \mathbf{m}_1) L_2(\log f) \\ &= D_2 \int d\nu f (-\mathbf{m}_1 \mathbf{m}_3 - \mathbf{m}_3 \mathbf{m}_1) (-\mathbf{b} \cdot \mathbf{m}_3 - B_1 : (\mathbf{m}_1 \mathbf{m}_3 + \mathbf{m}_3 \mathbf{m}_1)) \\ &= D_2 [\mathbf{b} \cdot \langle \mathbf{m}_3 (\mathbf{m}_3 \mathbf{m}_1 + \mathbf{m}_1 \mathbf{m}_3) \rangle + B_1 : \langle (\mathbf{m}_1 \mathbf{m}_3 + \mathbf{m}_3 \mathbf{m}_1) (\mathbf{m}_1 \mathbf{m}_3 + \mathbf{m}_3 \mathbf{m}_1) \rangle].\end{aligned}\tag{B.2}$$

Now we can rewrite

$$\begin{aligned}-\mathcal{M}_{\mathbf{p}} &= D_2 [\mu_{\mathbf{p}} \cdot \langle \mathbf{m}_3 \mathbf{m}_3 \rangle + \mu_{Q_1} : (\langle \mathbf{m}_1 \mathbf{m}_3 \mathbf{m}_3 \rangle + \langle \mathbf{m}_3 \mathbf{m}_1 \mathbf{m}_3 \rangle)] \\ &\quad + D_3 [\mu_{\mathbf{p}} \cdot \langle \mathbf{m}_2 \mathbf{m}_2 \rangle + (\mu_{Q_1} - \mu_{Q_2}) : (\langle \mathbf{m}_1 \mathbf{m}_2 \mathbf{m}_2 \rangle + \langle \mathbf{m}_2 \mathbf{m}_1 \mathbf{m}_2 \rangle)]. \\ -\mathcal{M}_{Q_1} &= D_2 [\mu_{\mathbf{p}} \cdot (\langle \mathbf{m}_3 \mathbf{m}_3 \mathbf{m}_1 \rangle + \langle \mathbf{m}_3 \mathbf{m}_1 \mathbf{m}_3 \rangle) \\ &\quad + \mu_{Q_1} : \langle (\mathbf{m}_1 \mathbf{m}_3 + \mathbf{m}_3 \mathbf{m}_1) (\mathbf{m}_1 \mathbf{m}_3 + \mathbf{m}_3 \mathbf{m}_1) \rangle] \\ &\quad + D_3 [\mu_{\mathbf{p}} \cdot (\langle \mathbf{m}_2 \mathbf{m}_2 \mathbf{m}_1 \rangle + \langle \mathbf{m}_2 \mathbf{m}_1 \mathbf{m}_2 \rangle) \\ &\quad + (\mu_{Q_1} - \mu_{Q_2}) : \langle (\mathbf{m}_1 \mathbf{m}_2 + \mathbf{m}_2 \mathbf{m}_1) (\mathbf{m}_1 \mathbf{m}_2 + \mathbf{m}_2 \mathbf{m}_1) \rangle]. \\ -\mathcal{M}_{Q_2} &= D_1 \mu_{Q_2} : \langle (\mathbf{m}_2 \mathbf{m}_3 + \mathbf{m}_3 \mathbf{m}_2) (\mathbf{m}_2 \mathbf{m}_3 + \mathbf{m}_3 \mathbf{m}_2) \rangle \\ &\quad + D_3 [-\mu_{\mathbf{p}} \cdot (\langle \mathbf{m}_2 \mathbf{m}_2 \mathbf{m}_1 \rangle + \langle \mathbf{m}_2 \mathbf{m}_1 \mathbf{m}_2 \rangle) \\ &\quad - (\mu_{Q_1} - \mu_{Q_2}) : \langle (\mathbf{m}_1 \mathbf{m}_2 + \mathbf{m}_2 \mathbf{m}_1) (\mathbf{m}_1 \mathbf{m}_2 + \mathbf{m}_2 \mathbf{m}_1) \rangle]. \\ \mathcal{V}_{\mathbf{p}} &= \kappa : \left[\langle \mathbf{m}_1 \mathbf{m}_3 \mathbf{m}_3 \rangle + \frac{I_{22}}{I_{11} + I_{22}} \langle \mathbf{m}_1 \mathbf{m}_2 \mathbf{m}_2 \rangle - \frac{I_{11}}{I_{11} + I_{22}} \langle \mathbf{m}_2 \mathbf{m}_1 \mathbf{m}_2 \rangle \right]. \\ (\mathcal{N}_{\mathbf{p}})_{\alpha} &= \partial_i \left(\partial_j (\mu_{\mathbf{p}})_k \sum_{\sigma=1}^3 \gamma_{\sigma} \langle m_{1k} m_{1\alpha} m_{\sigma i} m_{\sigma j} \rangle \right. \\ &\quad + \partial_j (\mu_{Q_1})_{kl} \sum_{\sigma=1}^3 \gamma_{\sigma} \langle m_{1k} m_{1l} m_{1\alpha} m_{\sigma i} m_{\sigma j} \rangle \\ &\quad \left. + \partial_j (\mu_{Q_2})_{kl} \sum_{\sigma=1}^3 \gamma_{\sigma} \langle m_{2k} m_{2l} m_{1\alpha} m_{\sigma i} m_{\sigma j} \rangle \right).\end{aligned}$$

$$\begin{aligned}
(\mathcal{N}_{Q_1})_{\alpha\beta} = & \partial_i \left(\partial_j (\mu_{\mathbf{p}})_k \sum_{\sigma=1}^3 \gamma_{\sigma} \langle \mathbf{m}_{1k} \mathbf{m}_{1\alpha} \mathbf{m}_{1\beta} \mathbf{m}_{\sigma i} \mathbf{m}_{\sigma j} \rangle \right. \\
& + \partial_j (\mu_{Q_1})_{kl} \sum_{\sigma=1}^3 \gamma_{\sigma} \langle \mathbf{m}_{1k} \mathbf{m}_{1l} \mathbf{m}_{1\alpha} \mathbf{m}_{1\beta} \mathbf{m}_{\sigma i} \mathbf{m}_{\sigma j} \rangle \\
& \left. + \partial_j (\mu_{Q_2})_{kl} \sum_{\sigma=1}^3 \gamma_{\sigma} \langle \mathbf{m}_{2k} \mathbf{m}_{2l} \mathbf{m}_{1\alpha} \mathbf{m}_{1\beta} \mathbf{m}_{\sigma i} \mathbf{m}_{\sigma j} \rangle \right). \\
(\mathcal{N}_{Q_2})_{\alpha\beta} = & \partial_i \left(\partial_j (\mu_{\mathbf{p}})_k \sum_{\sigma=1}^3 \gamma_{\sigma} \langle \mathbf{m}_{1k} \mathbf{m}_{2\alpha} \mathbf{m}_{2\beta} \mathbf{m}_{\sigma i} \mathbf{m}_{\sigma j} \rangle \right. \\
& + \partial_j (\mu_{Q_1})_{kl} \sum_{\sigma=1}^3 \gamma_{\sigma} \langle \mathbf{m}_{1k} \mathbf{m}_{1l} \mathbf{m}_{2\alpha} \mathbf{m}_{2\beta} \mathbf{m}_{\sigma i} \mathbf{m}_{\sigma j} \rangle \\
& \left. + \partial_j (\mu_{Q_2})_{kl} \sum_{\sigma=1}^3 \gamma_{\sigma} \langle \mathbf{m}_{2k} \mathbf{m}_{2l} \mathbf{m}_{2\alpha} \mathbf{m}_{2\beta} \mathbf{m}_{\sigma i} \mathbf{m}_{\sigma j} \rangle \right).
\end{aligned}$$

Meanwhile, we rewrite the elastic stress as

$$\begin{aligned}
\tau_e = & ck_B T \{ \mu_{Q_2} : \langle (\mathbf{m}_2 \mathbf{m}_3 + \mathbf{m}_3 \mathbf{m}_2) \mathbf{m}_2 \mathbf{m}_3 \rangle + \mu_{\mathbf{p}} \cdot \langle \mathbf{m}_3 \mathbf{m}_1 \mathbf{m}_3 \rangle \\
& + \mu_{Q_1} : \langle (\mathbf{m}_1 \mathbf{m}_3 + \mathbf{m}_3 \mathbf{m}_1) \mathbf{m}_1 \mathbf{m}_3 \rangle \\
& + \frac{1}{I_{11} + I_{22}} [\mu_{\mathbf{p}} \cdot \langle \mathbf{m}_2 (I_{22} \mathbf{m}_1 \mathbf{m}_2 - I_{11} \mathbf{m}_2 \mathbf{m}_1) \rangle \\
& + (\mu_{Q_1} - \mu_{Q_2}) : \langle (\mathbf{m}_1 \mathbf{m}_2 + \mathbf{m}_2 \mathbf{m}_1) (I_{22} \mathbf{m}_1 \mathbf{m}_2 - I_{11} \mathbf{m}_2 \mathbf{m}_1) \rangle] \}. \quad (\text{B.3})
\end{aligned}$$

From the above equations, we deduce (3.21).

C Kirkwood theory

We describe how to calculate the spatial diffusion coefficient matrix \mathbf{J} using the Kirkwood theory. Assume that the molecule consists of N spheres. Denote by \mathbf{F}_i the force exerted on the sphere i due to hydrodynamic interaction. The Kirkwood theory gives

$$\mathbf{V}_i = \sum_j H_{ij} \mathbf{F}_j, \quad (\text{C.1})$$

where

$$H_{ij} = \frac{1}{8\pi\eta_0 |\hat{\mathbf{r}}_{ij}|} \left(I + \frac{\hat{\mathbf{r}}_{ij} \hat{\mathbf{r}}_{ij}}{|\hat{\mathbf{r}}_{ij}|^2} \right), \quad \hat{\mathbf{r}}_{ij} = \hat{\mathbf{r}}_j - \hat{\mathbf{r}}_i, \quad j \neq i. \quad (\text{C.2})$$

For $j = i$, we adopt the approximation $H_{ii} = I/\tau$ [10], where I is the identity matrix. We choose $\tau = 32\pi\eta_0 D$. Suppose that a molecule is undergoing a translation in the quiescent fluid with the velocity \mathbf{V} . Then $\mathbf{V}_i = \mathbf{V}$. On the other hand, the total hydrodynamic force shall be identical to the force that stems from the thermodynamic potential. Thus we have

$$\sum_i \mathbf{F}_i = -\nabla \mu. \quad (\text{C.3})$$

From (C.1) and (C.3), we can deduce the relation of \mathbf{V} and $\nabla\mu$. Define $H \in \mathbb{R}^{3N \times 3N}$, $L \in \mathbb{R}^{3 \times 3N}$ and $\mathbf{F} \in \mathbb{R}^{3N}$ by

$$H = \begin{pmatrix} H_{11} & \dots & H_{1N} \\ \vdots & & \vdots \\ H_{N1} & \dots & H_{NN} \end{pmatrix}, \quad L = \underbrace{(I, I, \dots, I)}_N, \quad \mathbf{F} = \begin{pmatrix} \mathbf{F}_1 \\ \vdots \\ \mathbf{F}_N \end{pmatrix}.$$

Then we can rewrite (C.1) and (C.3) as

$$H\mathbf{F} = L^T\mathbf{V}, \quad L\mathbf{F} = -\nabla\mu.$$

Therefore, we can solve that

$$\mathbf{V} = -(LH^{-1}L^T)^{-1}\nabla\mu.$$

Thus, $\mathbf{J} = (LH^{-1}L^T)^{-1}$.

For bent-core molecules, we use a discrete version of (2.37), namely to view the molecule as consisting of $1 + N = 1 + 1/\eta$ spheres located at

$$\hat{\mathbf{r}}_j = l\left(\frac{1}{4} - |s_j|\right) \cos \frac{\theta}{2} \mathbf{m}_1 + ls_j \sin \frac{\theta}{2} \mathbf{m}_2, \quad (\text{C.4})$$

where $s_j = j/N$, $-N/2 \leq j \leq N/2$. Using this molecular architecture we arrive at (2.41).

D Symmetry of the molecular model in homogeneous case

We investigate the Smochulowski equation in the shear flow,

$$\frac{\partial f(P, t)}{\partial t} = L \cdot [(D_0 \mathbf{I}^{-1})(k_B T L f + f L V)] - L \cdot (g f), \quad (\text{D.1})$$

where g is given by (2.34), V is given by (3.4) and (3.1)-(3.3) without gradient terms. We will prove that if the equality

$$f(P(\alpha, \beta, \gamma), t) = f(P(\alpha, \beta, \gamma + \pi), t) = f(P(\pi - \alpha, \beta + \pi, \pi - \gamma), t) = f(P(\pi - \alpha, \beta, -\gamma), t)$$

holds for $t = 0$, then it holds for $t > 0$.

We only prove the first equality, because the other two follow exactly the same way. By (2.7), for arbitrary u , we have

$$\begin{aligned} (L_1 u)(P(\alpha, \beta, \gamma), t) &= L_1 \left(u(P(\alpha, \beta, \gamma + \pi), t) \right), \\ (L_2 u)(P(\alpha, \beta, \gamma), t) &= -L_2 \left(u(P(\alpha, \beta, \gamma + \pi), t) \right), \\ (L_3 u)(P(\alpha, \beta, \gamma), t) &= -L_3 \left(u(P(\alpha, \beta, \gamma + \pi), t) \right). \end{aligned}$$

We then examine the symmetry of right-hand terms at $t = 0$. By the symmetry of f , we also have $V(P(\alpha, \beta, \gamma), 0) = V(P(\alpha, \beta, \gamma + \pi), 0)$. Thus, we can verify that for the diffusion term,

$$\left[L \cdot \left((D_0 \mathbf{I}^{-1})(k_B T L f + f L V) \right) \right] (P(\alpha, \beta, \gamma), 0)$$

$$= \left[L \cdot \left((D_0 \mathbf{I}^{-1})(k_B T L f + f L V) \right) \right] (P(\alpha, \beta, \gamma + \pi), 0).$$

For the convection term, write $\mathbf{g} = \sum_{i=1}^3 (\kappa : \alpha_i) \mathbf{m}_i$. It is straightforward to verify that

$$\begin{aligned} \alpha_1(P(\alpha, \beta, \gamma), 0) &= \alpha_1(P(\alpha, \beta, \gamma + \pi), 0), \\ \alpha_2(P(\alpha, \beta, \gamma), 0) &= -\alpha_2(P(\alpha, \beta, \gamma + \pi), 0), \\ \alpha_3(P(\alpha, \beta, \gamma), 0) &= -\alpha_3(P(\alpha, \beta, \gamma + \pi), 0). \end{aligned}$$

Hence,

$$[L \cdot (\mathbf{g}f)](P(\alpha, \beta, \gamma), 0) = [L \cdot (\mathbf{g}f)](P(\alpha, \beta, \gamma + \pi), 0).$$

Therefore, $f(P(\alpha, \beta, \gamma), t)$ and $f(P(\alpha, \beta, \gamma + \pi), t)$ are governed by the same equation. Since they are equal at $t = 0$, it is also the case for any $t > 0$.

Acknowledgments. Pingwen Zhang is partially supported by National Natural Science Foundation of China (Grant No. 11421101 and 11421110001).

References

- [1] B. R. Acharya, A. Primak, and S. Kumar. Biaxial nematic phase in bent-core thermotropic mesogens. *Phys. Rev. Lett.*, 92:145506, 2004.
- [2] S. G. Advani and C. L. Tucker III. The use of tensors to describe and predict fiber orientation in short fiber composites. *J. Rheol.*, 31(8):751–784, 1987.
- [3] S. G. Advani and C. L. Tucker III. Closure approximations for three-dimensional structure tensors. *J. Rheol.*, 34(3):367–386, 1990.
- [4] A. N. Beris and B. J. Edwards. *Thermodynamics of Flowing Systems with Internal Microstructure*. Oxford University Press, 1994.
- [5] F. Bisi, E. G. Virga, and E. C. Gartland et al. Universal mean-field phase diagram for biaxial nematics obtained from a minimax principle. *Phys. Rev. E*, 73:051709, 2006.
- [6] V. Borshch, Y.-K. Kim, J. Xiang, M. Gao, A. Jákli, V. P. Panov, J. K. Vij, C. T. Imrie, M. G. Tamba, G. H. Mehl, and O. D. Lavrentovich. Nematic twist-bend phase with nanoscale modulation of molecular orientation. *Nat. Commun.*, 4:2635, 2013.
- [7] H. Brand and H. Pleiner. Hydrodynamics of biaxial discotics. *Phys. Rev. A*, 24:2777, 1981.
- [8] C. V. Chaubal and L. G. Leal. A closure approximation for liquid-crystalline polymer models based on parametric density estimation. *J. Rheol.*, 42(1):177–201, 1998.
- [9] D. Chen, J. H. Porada, J. B. Hooper, A. Klittnick, Y. Shen, M. R. Tuchband, E. Korblova, D. Bedrov, D. M. Walba, M. A. Glaser, J. E. MacLennan, and N. A. Clark. Chiral heliconical ground state of nanoscale pitch in a nematic liquid crystal of achiral molecular dimers. *Proc. Natl. Acad. Sci. USA*, 110:15931, 2013.

- [10] M. Doi and S. F. Edwards. *The Theory of Polymer Dynamics*. Oxford University Press, 1986.
- [11] J. Feng, C. V. Chaubal, and L. G. Leal. Closure approximations for the Doi theory: Which to use in simulating complex flows of liquid-crystalline polymers? *J. Rheol.*, 42(5):1095–1119, 1998.
- [12] M. G. Forest, Q. Wang, and R. Zhou. The flow-phase diagram of Doi–Hess theory for sheared nematic polymers II: finite share rates. *Rheol. Acta.*, 44(1):80–93, 2004.
- [13] M. G. Forest, Q. Wang, and R. Zhou. The weak shear kinetic phase diagram for nematic polymers. *Rheol. Acta.*, 43(1):17–37, 2004.
- [14] M. G. Forest, R. Zhou, and Q. Wang. Kinetic structure simulations of nematic polymers in plane Couette cells. II: in-plane structure transitions. *Multiscale Model. Simul.*, 4(4):1280–1304, 2005.
- [15] C. Greco and A. Ferrarini. Entropy-Driven Chiral Order in a System of Achiral Bent Particles. *Phys. Rev. Lett.*, 115:147805, 2015.
- [16] J. Han, Y. Luo, W. Wang, P. Zhang, and Z. Zhang. From microscopic theory to macroscopic theory: a systematic study on modeling for liquid crystals. *Arch. Rat. Mech. Anal.*, 215:741, 2015.
- [17] E. J. Hinch and L. G. Leal. Constitutive equations in suspension mechanics. Part II. Approximation forms for a suspension of rigid particles affected by Brownian rotations. *J. Fluid Mech.*, 76:187–208, 1976.
- [18] P. Ilg, I. V. Karlin, M. Kröger, and H. C. Öttinger. Canonical distribution functions in polymer dynamics. (II). Liquid-crystalline polymers. *Physica A*, 319:134–150, 2003.
- [19] J. S. Cintra, Jr. and C. L. Tucker III. Orthotropic closure approximations for flow-induced fiber orientation. *J. Rheol.*, 39(6):1095, 1995.
- [20] R. G. Larson. Arrested tumbling in shearing flows of liquid-crystal polymers. *Macromolecules*, 23:3983–3992, 1990.
- [21] R. G. Larson and H. C. Öttinger. Effect of molecular elasticity on out-of-plane orientations in shearing flows of liquid-crystalline polymers. *Macromolecules*, 24:6270–6282, 1991.
- [22] F. M. Leslie. Theory of flow phenomena in liquid crystals. *Adv. Liq. Cryst.*, 4:1–81, 1979.
- [23] M. Liu. Hydrodynamic theory of biaxial nematics. *Phys. Rev. A*, 24:2720, 1981.
- [24] L. A. Madsen, T. J. Dingemans, M. Nakata, and E. T. Samulski. Thermotropic biaxial nematic liquid crystals. *Phys. Rev. Lett.*, 92:145505, 2004.
- [25] G. Marrucci and F. Greco. A molecular approach to the polydomain structure of LCPs in weak shear flows. *J. Non-Newtonian Fluid Mech.*, 44:1–13, 1992.

- [26] C. Meyer, G. R. Luckhurst, and I. Dozov. Flexoelectrically Driven Electroclinic Effect in the Twist-Bend Nematic Phase of Achiral Molecules with Bent Shapes. *Phys. Rev. Lett.*, 111:067801, 2013.
- [27] T. Qian and P. Sheng. Generalized hydrodynamic equations for nematic liquid crystals. *Phys. Rev. E*, 58:7475–7485, 1998.
- [28] W. M. Saslow. Hydrodynamics of biaxial nematics with arbitrary nonsingular textures. *Phys. Rev. A*, 25:3350, 1982.
- [29] S. M. Shamid, D. W. Allender, and J. V. Selinger. Predicting a Polar Analog of Chiral Blue Phases in Liquid Crystals. *Phys. Rev. Lett.*, 113:237801, 2014.
- [30] S. M. Shamid, S. Dhakal, and J. V. Selinger. Statistical mechanics of bend flexoelectricity and the twist-bend phase in bent-core liquid crystals. *Phys. Rev. E*, 87:052503, 2013.
- [31] S. Sircar, J. Li, and Q. Wang. Biaxial phases of bent-core liquid crystal polymers in shear flows. *Comm. Math. Sci.*, 8:697–720, 2010.
- [32] S. Sircar and Q. Wang. Shear-induced mesostructures in biaxial liquid crystals. *Phys. Rev. E*, 78:061702, 2008.
- [33] S. Sircar and Q. Wang. Dynamics and rheology of biaxial liquid crystal polymers in shear flow. *J. Rheol.*, 53:819–858, 2009.
- [34] E. G. Virga. Double-well elastic theory for twist-bend nematic phases. *Phys. Rev. E*, 89:052502, 2014.
- [35] Q. Wang. Comparative studies on closure approximations in flows of liquid crystal polymers: I. elongational flows. *J. Non-Newtonian Fluid Mech.*, 72(2-3):141–162, 1997.
- [36] Q. Wang, W. E, C. Liu, and P. Zhang. Kinetic theory for flows of nonhomogeneous rodlike liquid crystalline polymers with a nonlocal intermolecular potential. *Phys. Rev. E*, 65:051504, 2002.
- [37] E. P. Wigner. *Group Theory and its Application to the Quantum Mechanics of Atomic Spectra*. Academic Press, New York, 1959.
- [38] J. Xu, F. Ye, and P. Zhang. A tensor model for nematic phases of bent-core molecules based on molecular theory. *Submitted to Multiscale Model. Simul.*, arXiv:1408:3722v2, 2016.
- [39] J. Xu and P. Zhang. From microscopic theory to macroscopic theory — symmetries and order parameters of rigid molecules. *Sci. China Math.*, 57:443–468, 2014.
- [40] H. Yu, G. Ji, and P. Zhang. A Nonhomogeneous Kinetic Model of Liquid Crystal Polymers and Its Thermodynamic Closure Approximation. *Commun. Comput. Phys.*, 7(2):383–402, 2010.
- [41] H. Yu and P. Zhang. A kinetic hydrodynamic simulation of microstructure of liquid crystal polymers in plane shear flow. *J. Non-Newtonian Fluid Mech.*, 141:116–127, 2007.

- [42] R. Zhou, M. G. Forest, and Q. Wang. Kinetic structure simulations of nematic polymers in plane couette cells. I: the algorithm and benchmarks. *Multiscale Model. Simul.*, 3(4):853–870, 2005.